
Report of the Quark Flavor Physics Working Group

1 **Conveners: J.N. Butler, Z. Ligeti, J.L. Ritchie**

2 **Task Force leaders:**

3 **V. Cirigliano, S. Kettell (Kaons); R. Briere, A.A. Petrov (Charm);**

4 **A. Schwartz, T. Skwarnicki, J. Zupan (B physics);**

5 **N. Christ, S.R. Sharpe, R.S. Van de Water (Lattice QCD)**

6 W. Altmannshofer, N. Arkani-Hamed, M. Artuso, D.M. Asner, C. Bernard, A.J. Bevan, M. Blanke,
7 G. Bonvicini, T.E. Browder, D.A. Bryman, P. Campana, R. Cenci, D. Cline, J. Comfort,
8 D. Cronin-Hennessy, A. Datta, S. Dobbs, M. Duraisamy, A.X. El-Khadra, J.E. Fast, R. Forty, K.T. Flood,
9 T. Gershon, Y. Grossman, B. Hamilton, C.T. Hill, R.J. Hill, D.G. Hitlin, D.E. Jaffe, A. Jawahery,
10 C.P. Jessop, A.L. Kagan, D.M. Kaplan, M. Kohl, P. Krizan, A.S. Kronfeld, K. Lee, L.S. Littenberg,
11 D.B. MacFarlane, P.B. Mackenzie, B.T. Meadows, J. Olsen, M. Papucci, Z. Parsa, G. Paz, G. Perez,
12 L.E. Pilonen, K. Pitts, M.V. Purohit, B. Quinn, B.N. Ratcliff, D.A. Roberts, J.L. Rosner, P. Rubin,
13 J. Seeman, K.K. Seth, B. Schmidt, A. Schopper, M.D. Sokoloff, A. Soni, K. Stenson, S. Stone, R. Sundrum,
14 R. Tschirhart, A. Vainshtein, Y.W. Wah, G. Wilkinson, M.B. Wise, E. Worcester, J. Xu, T. Yamanaka

15 16 1.1 Introduction

17 This report, from the Quark Flavor Physics working group, describes the physics case for precision studies of
18 flavor-changing interactions of bottom, charm, and strange quarks, and it discusses the experimental program
19 needed to exploit these physics opportunities. It also discusses the role of theory and the importance of lattice
20 QCD to future progress in this field. The report is the result of a process that began before Snowmass, in the
21 fall of 2011 with the DOE-sponsored workshop on Fundamental Physics at the Intensity Frontier (Rockville,
22 MD). The Heavy Quarks working group from that workshop continued into the Snowmass process, albeit
23 with a change of name to Quark Flavor Physics to better reflect our emphasis on quark flavor mixing. The
24 Heavy Quarks report [1] from that workshop provided a starting point for our Snowmass efforts.

25 With the initiation of the Snowmass process, our working group grew. Also, four Task Forces were organized
26 to focus on four closely related, but distinct, areas of effort in quark-flavor physics: kaons, charm, B -physics,
27 and lattice QCD. Our working group had physical meetings during the Community Planning Meeting at
28 Fermilab (October, 2012), at the Intensity Frontier Workshop at Argonne (April, 2013), and at Snowmass
29 itself at the University of Minnesota (July, 2013). Consequently, this report is the culmination of discussions
30 that were conducted over a period of almost two years.

31 This report describes the physics case for quark-flavor physics, and it represents the aspirations of a
32 substantial community of physicists in the U.S. who are interested in this physics. This report is not a
33 review of quark-flavor physics, and no attempt has been made to provide complete references to prior work.
34 Rather, it focuses on the opportunities for spectacular discoveries during the remainder of this decade and
35 during the next decade, made possible by the extraordinary reach to high mass scales that is possible in
36 quark-flavor physics experiments.

37 Nevertheless, before looking forward, it provides useful context to briefly review some history. In the 1990's,
38 the U.S. was the leader both on the Energy Frontier and in quark flavor-physics experiments at the Intensity
39 Frontier. B physics was still dominated by the CLEO experiment for most of that decade. The most sensitive
40 rare K decay experiments performed to date were then underway at the Brookhaven AGS, including an
41 experiment that made the first observation of the extremely rare $K^+ \rightarrow \pi^+ \nu \bar{\nu}$ decay, and a fixed-target
42 experiment using the Tevatron at Fermilab was underway that observed direct CP violation in $K_L^0 \rightarrow \pi\pi$
43 decays. Toward the end of that decade, the asymmetric e^+e^- B factories began running at SLAC and KEK,
44 leading to increases in the size of B meson data sets by two orders of magnitude and also opening the door to
45 measurements of time-dependent CP asymmetries, which provided the experimental basis for the 2008 Nobel
46 Prize. In the midst of this success, a number of new and ambitious quark-flavor initiatives were put forward
47 in the U.S. These included the BTeV proposal which would have used the Tevatron collider for B physics,
48 the CKM proposal which would have made the first high-statistics measurement of $K^+ \rightarrow \pi^+ \nu \bar{\nu}$ using
49 the Fermilab Main Injector, and the RSVP proposal which included an experiment (KOPIO) to measure
50 $K_L^0 \rightarrow \pi^0 \nu \bar{\nu}$ at the Brookhaven AGS. After lengthy consideration in an environment characterized by flat
51 budgets and a predilection for a fast start on the International Linear Collider on U.S. soil, all of these
52 initiatives were ultimately terminated. Also, as accelerator breakthroughs capable of increasing B -factory
53 luminosity by more than another order of magnitude were made, the opportunity to upgrade the PEP-II
54 B factory at SLAC was not pursued. This history is relevant in order to stress that the U.S. has been a
55 leader in flavor-physics experiments — involving a vigorous community — until very recently. Nonetheless,
56 this sequence of events inevitably encouraged many in the flavor-physics community in the U.S. to migrate
57 elsewhere, most often to ATLAS or CMS at the LHC.

58 In spite of these developments in the U.S., strong physics imperatives have motivated a rich quark flavor
59 physics program that is flourishing around the world. Kaon experiments, B -physics experiments, and charm
60 experiments are running and under construction in Asia and Europe. Indeed, CERN — the laboratory that
61 now owns the Energy Frontier — is also the home of a running B -physics experiment (LHCb), which has
62 a clear upgrade path, and a rare K decay experiment (NA62), focusing on $K^+ \rightarrow \pi^+ \nu \bar{\nu}$, which will begin
63 taking data near the end of 2014. This reflects the world-wide consensus that flavor-physics experiments are
64 critical to progress in particle physics.

65 Looking forward, it is clear that there continues to be strong interest and a potentially substantial community
66 in the U.S. for an Intensity Frontier flavor-physics program. The motivation for this program can be described
67 very simply. If the LHC observes new high-mass states, it will be necessary to distinguish among models
68 proposed to explain them. This will require tighter constraints from the flavor sector, which can come from
69 more precise experiments using strange, charm, and bottom quark systems. If the LHC does not make
70 such discoveries, then the ability of precision flavor-physics experiments to probe mass scales far above LHC,
71 through virtual effects, is the best hope to see signals that may point toward the next energy scale to explore.

72 In the following sections of this report, we describe the general physics case for quark-flavor physics, followed
73 by the reports of each of the Task Forces. The Task Forces were in communication with each other, but
74 worked independently on these reports. Finally, this report concludes with a discussion of how the U.S.
75 high-energy physics program can, at relatively modest cost compared to most other initiatives, participate
76 in critical flavor-physics experiments offshore and regain some of its leadership status by executing a program
77 of rare kaon decay experiments at Fermilab.

1.2 Quark Flavor as a Tool for Discovery

An essential feature of flavor physics experiments is their ability to probe very high mass scales, beyond the energies accessible in collider experiments. In addition, flavor physics can teach us about properties of TeV-scale new physics, which cannot be learned from the direct production of new particles at the LHC. This is because quantum effects allow virtual particles to modify the results of precision measurements in ways that reveal the underlying physics. (The determination of the t - s and t - d couplings in the standard model (SM) exemplifies how measurements of some properties of heavy particles may only be possible in flavor physics.) Even as the LHC embarks on probing the TeV scale, the ongoing and planned precision flavor physics experiments are sensitive to beyond standard model (BSM) interactions at mass scales which are higher by several orders of magnitude. These experiments will provide essential constraints and complementary information on the structure of models put forth to explain any discoveries at LHC, and they have the potential to reveal new physics that is inaccessible to the LHC.

Throughout the history of particle physics discoveries made in studies of rare processes have led to new and deeper understanding of nature. A classic example is beta decay, which foretold the electroweak mass scale and the ultimate observation of the W boson. Results from kaon decay experiments were crucial for the development of the standard model: the discovery of CP violation in $K_L^0 \rightarrow \pi^+ \pi^-$ decay ultimately pointed toward the three-generation CKM model [2, 3], the absence of strangeness-changing neutral current decays (i.e., the suppression of $K_L^0 \rightarrow \mu^+ \mu^-$ with respect to $K^+ \rightarrow \mu^+ \nu$) led to the prediction of a fourth quark [4] (charm), and the measured value of the $K_L - K_S$ mass difference made it possible to predict the charm quark mass [5, 6] before charm particles were directly detected. The larger than expected $B_H - B_L$ mass difference foretold the high mass of the top quark. Precision measurements of time-dependent CP-violating asymmetries in B -meson decays in the BABAR and Belle experiments firmly established the CKM phase as the dominant source of CP violation observed to date in flavor-changing processes — leading to the 2008 Nobel Prize for Kobayashi and Maskawa. At the same time, corrections to the SM at the tens of percent level are still allowed, and many extensions of the SM proposed to solve the hierarchy problem are likely to give rise to changes in flavor physics that may be observed in the next generation of experiments.

1.2.1 Strange, Charm, and Bottom Quarks as Probes for New Physics

In the past decade our understanding of flavor physics has improved significantly due to the $e^+ e^- B$ factories, BABAR, Belle, CLEO, the Tevatron experiments, and most recently LHCb. While kaon physics was crucial for the development of the SM, and has provided some of the most stringent constraints on BSM physics since the 1960s, precision tests of the CKM picture of CP violation in the kaon sector alone have been hindered by theoretical uncertainties in calculating direct CP violation (ϵ'_K). The B factories and LHCb provided many stringent tests by precisely measuring numerous CP-violating and CP-conserving quantities, which in the SM are determined in terms of just a few parameters, but are sensitive to different possible BSM contributions. The consistency of the measurements and their agreement with CP violation in $K^0 - \bar{K}^0$ mixing, ϵ_K , and with the SM predictions (shown in the left plot in Fig. 1-1) strengthened the “new physics flavor problem”. It is the tension between the relatively low (TeV) scale required to stabilize the electroweak scale, and the high scale that is seemingly required to suppress BSM contributions to flavor-changing processes. This problem arises because the SM flavor structure is very special, containing small mixing angles, and because of additional strong suppressions of flavor-changing neutral-current (FCNC) processes. Any TeV-scale new physics must preserve these features, which are crucial to explain the observed pattern of weak decays.

Operator	Bounds on Λ [TeV] ($C = 1$)		Bounds on C ($\Lambda = 1$ TeV)		Observables
	Re	Im	Re	Im	
$(\bar{s}_L \gamma^\mu d_L)^2$	9.8×10^2	1.6×10^4	9.0×10^{-7}	3.4×10^{-9}	$\Delta m_K; \epsilon_K$
$(\bar{s}_R d_L)(\bar{s}_L d_R)$	1.8×10^4	3.2×10^5	6.9×10^{-9}	2.6×10^{-11}	$\Delta m_K; \epsilon_K$
$(\bar{c}_L \gamma^\mu u_L)^2$	1.2×10^3	2.9×10^3	5.6×10^{-7}	1.0×10^{-7}	$\Delta m_D; q/p , \phi_D$
$(\bar{c}_R u_L)(\bar{c}_L u_R)$	6.2×10^3	1.5×10^4	5.7×10^{-8}	1.1×10^{-8}	$\Delta m_D; q/p , \phi_D$
$(\bar{b}_L \gamma^\mu d_L)^2$	6.6×10^2	9.3×10^2	2.3×10^{-6}	1.1×10^{-6}	$\Delta m_{B_d}; S_{\psi K_S}$
$(\bar{b}_R d_L)(\bar{b}_L d_R)$	2.5×10^3	3.6×10^3	3.9×10^{-7}	1.9×10^{-7}	$\Delta m_{B_d}; S_{\psi K_S}$
$(\bar{b}_L \gamma^\mu s_L)^2$	1.4×10^2	2.5×10^2	5.0×10^{-5}	1.7×10^{-5}	$\Delta m_{B_s}; S_{\psi \phi}$
$(\bar{b}_R s_L)(\bar{b}_L s_R)$	4.8×10^2	8.3×10^2	8.8×10^{-6}	2.9×10^{-6}	$\Delta m_{B_s}; S_{\psi \phi}$

Table 1-1. Bounds on some $\Delta F = 2$ operators of the form $(C/\Lambda^2)\mathcal{O}$, with \mathcal{O} given in the first column. The bounds on Λ assume $C = 1$, the bounds on C assume $\Lambda = 1$ TeV. (From Ref. [7].)

119 The motivation for a broad program of precision flavor physics measurements has gotten even stronger in
120 light of the first LHC run. With the discovery of a new particle whose properties are similar to the SM Higgs
121 boson, but no sign of other high-mass states, the LHC has begun to test naturalness as a guiding principle
122 of BSM research. If the electroweak scale is unnatural, we have little information on the next energy scale
123 to explore (except for a hint at the TeV scale from dark matter, a few anomalous experimental results, and
124 neutrinos most likely pointing at a very high scale). The flavor physics program will explore much higher
125 scales than can be directly probed. However, if the electroweak symmetry breaking scale is stabilized by a
126 natural mechanism, new particles should be found at the LHC. Since the largest quantum correction to the
127 Higgs mass in the SM is due to the top quark, the new particles will likely share some properties of the SM
128 quarks, such as symmetries and interactions. Then they would provide a novel probe of the flavor sector,
129 and flavor physics and the LHC data would provide complementary information. Their combined study is
130 our best chance to learn more about the origin of both electroweak and flavor symmetry breaking.

131 Consider, for example, a model in which the only suppression of new flavor-changing interactions comes
132 from the large masses of the new particles that mediate them (at a scale $\Lambda \gg m_W$). Flavor physics,
133 in particular measurements of meson mixing and CP violation, put severe lower bounds on Λ . For some
134 of the most important four-quark operators contributing to the mixing of the neutral K , D , B , and B_s
135 mesons, the bounds on the coefficients C/Λ^2 are summarized in Table 1-1. For $C = 1$, they are at the
136 scale $\Lambda \sim (10^2 - 10^5)$ TeV. Conversely, for $\Lambda = 1$ TeV, the coefficients have to be very small. Therefore,
137 there is a tension. The hierarchy problem can be solved with new physics at $\Lambda \sim 1$ TeV. Flavor bounds,
138 however, require much larger scales, or tiny couplings. This tension implies that TeV-scale new physics
139 must have special flavor structures, e.g., possibly sharing some of the symmetries that shape the SM Yukawa
140 interactions. The new physics flavor puzzle is thus the question of why, and in what way, the flavor structure
141 of the new physics is non-generic. As a specific example, in a supersymmetric extension of the SM, there are
142 box diagrams with winos and squarks in the loops. The size of such contributions depends crucially on the
143 mechanism of SUSY breaking, which we would like to probe.

144 To be sensitive to BSM contributions to FCNC processes (where the SM is suppressed, but not absent), many
145 measurements need to be done, and it is only their combination that can reveal a signal. (There are some
146 exceptions, mainly processes forbidden in the SM, but considering only those would reduce the sensitivity
147 of the program to BSM physics.) To visualize the constraints from many measurements, it is convenient to

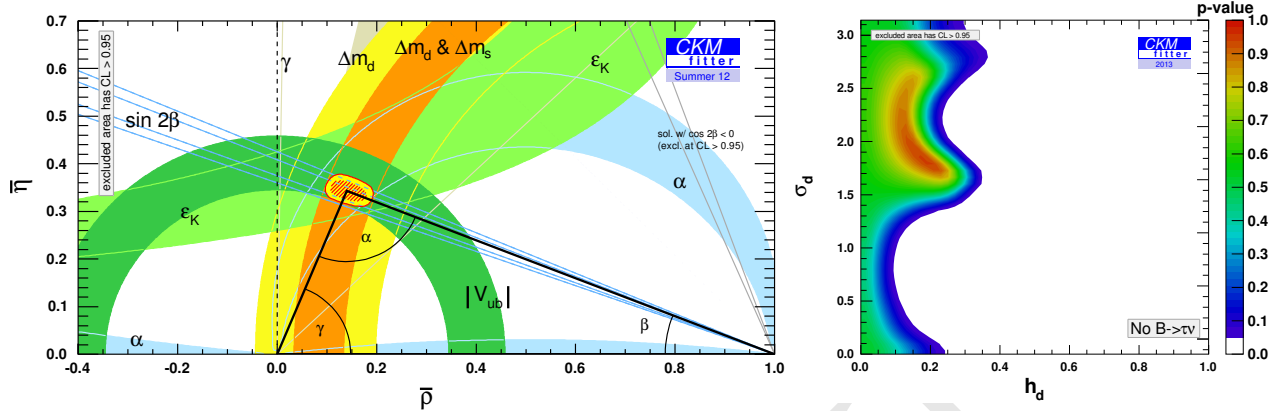


Figure 1-1. Left: Constraints on the apex of the unitarity triangle in the $\bar{\rho} - \bar{\eta}$ plane (at 95% CL) [8, 9]. Right: the allowed $h_d - \sigma_d$ new physics parameter space (see text) in $B^0 - \bar{B}^0$ mixing.

148 use the Wolfenstein parameterization [10] of the CKM matrix (for a review, see [11]),

$$V_{\text{CKM}} = \begin{pmatrix} V_{ud} & V_{us} & V_{ub} \\ V_{cd} & V_{cs} & V_{cb} \\ V_{td} & V_{ts} & V_{tb} \end{pmatrix} = \begin{pmatrix} 1 - \frac{1}{2}\lambda^2 & \lambda & A\lambda^3(\bar{\rho} - i\bar{\eta}) \\ -\lambda & 1 - \frac{1}{2}\lambda^2 & A\lambda^2 \\ A\lambda^3(1 - \bar{\rho} - i\bar{\eta}) & -A\lambda^2 & 1 \end{pmatrix} + \mathcal{O}(\lambda^4). \quad (1.1)$$

149 It exhibits the hierarchical structure of the CKM matrix by expanding in a small parameter, $\lambda \simeq 0.23$. The
 150 unitarity of this matrix in the SM implies many relations, such as that defining the “unitarity triangle”
 151 shown in Fig. 1-1, which arises from rescaling $V_{ud}V_{ub}^* + V_{cd}V_{cb}^* + V_{td}V_{tb}^* = 0$ by $V_{cd}V_{cb}^*$ and choosing two
 152 vertices of the resulting triangle to be $(0, 0)$ and $(1, 0)$.

153 As a result of second-order weak interaction processes, there are transitions between the neutral meson flavor
 154 eigenstates, so the physical mass eigenstates are their linear combinations, denoted as $|B_{H,L}\rangle = p|B^0\rangle \mp q|\bar{B}^0\rangle$.
 155 (The p and q parameters differ for the four neutral mesons, but the same notation is commonly used without
 156 distinguishing indices.) In a large class of models, the BSM physics modifies the mixing amplitude of neutral
 157 mesons, and leaves tree-level decays unaffected. This effect can be parameterized by just two real parameters
 158 for each mixing amplitude. For $B^0 - \bar{B}^0$ mixing, writing $M_{12} = M_{12}^{\text{SM}}(1 + h_d e^{2i\sigma_d})$, the constraints on h_d and
 159 σ_d are shown in the right plot in Fig. 1-1. (Evidence for $h_d \neq 0$ would rule out the SM.) Only in 2004, after
 160 the first significant constraints on γ and α from BABAR and Belle, did we learn that the BSM contribution
 161 to $B^0 - \bar{B}^0$ mixing must be less than the SM amplitude [12, 9]. The right plot in Fig. 1-1 shows that order
 162 20% corrections to $|M_{12}|$ are still allowed for (almost) any value of the phase of the new physics contribution,
 163 and if this phase is aligned with the SM ($\sigma_d = 0 \bmod \pi/2$), then the new physics contribution does not yet
 164 have to be much smaller than the SM one. Similar conclusions apply for B_s^0 and K^0 mixings [13, 14], as well
 165 as many other $\Delta F = 1$ FCNC transition amplitudes.

166 The fact that such large deviations from the SM are not yet excluded gives very strong motivations to
 167 continue flavor physics measurements in order to observe deviations from the SM predictions or establish an
 168 even stronger hierarchy between the SM and new physics contributions.

169 In considering the future program, the following issues [15] are of key importance:

- 170 1. What are the expected deviations from the SM predictions induced by new physics at the TeV scale?
 171 As explained above, TeV-scale new physics with generic flavor structure is ruled out by many orders
 172 of magnitude. However, sizable deviations from the SM are still allowed by the current bounds, and in
 173 many scenarios observable effects are expected.

174 2. What are the theoretical uncertainties?

175 These are highly process dependent. Some measurements are limited by theoretical uncertainties (due
176 to hadronic, strong interaction, effects), but in many key processes the theory uncertainties are very
177 small, below the expected sensitivity of future experiments.

178 3. In which processes will the sensitivity to BSM physics increase the most?

179 The useful data sets can increase by a factor of order 100 (in most cases 10–1000), and will probe
180 effects predicted by fairly generic BSM scenarios.

181 4. What will the measurements reveal, if deviations from the SM are [not] seen?

182 The flavor physics data will be complementary with the high- p_T part of the LHC program. The synergy
183 of measurements can reveal a lot about what the new physics at the TeV scale is, and what it is not.

184 This report concentrates on the physics and prospects of a subset of measurements, for which the answers
185 to these questions are the clearest, both in terms of theoretical cleanliness and experimental feasibility. The
186 experiments will enable many additional measurements which are not discussed here, some due to lack of
187 space, and some because they will be more important than can now be anticipated. (Recall that the best
188 measurements of the CKM angles α and γ at *BABAR* and *Belle* were not in formerly expected decay modes.)
189 While future theory progress is important, the value of more sensitive experiments is not contingent on it.

190 **1.2.2 The Role of Theory**

191 To find a convincing deviation from the SM, a new physics effect has to be several times larger than the
192 experimental uncertainty of the measurement and the theoretical uncertainty of the SM prediction. One
193 often distinguishes two kinds of theoretical uncertainties, perturbative and nonperturbative (this separation
194 is not unambiguous). Perturbative uncertainties come from the truncation of expansions in small (or not-so-
195 small) coupling constants, such as α_s at a few GeV scale. There are always higher order terms that have not
196 been computed. Nonperturbative effects arise because QCD becomes strongly interacting at low energies,
197 and these are often the limiting uncertainties. There are, nevertheless, several possibilities to get at the
198 fundamental physics in certain cases.

- 199 • For some observables the hadronic parameters (mostly) cancel, or can be extracted from data (e.g.,
200 using the measured $K \rightarrow \pi \ell \nu$ form factor to predict $K \rightarrow \pi \nu \bar{\nu}$, several methods to extract γ , etc.).
- 201 • In many cases, CP invariance of the strong interaction implies that the dominant hadronic physics
202 cancels, or is CKM suppressed (e.g., measuring β from $B \rightarrow \psi K_S$, and some other CP asymmetries).
- 203 • In some cases one can use symmetries of the strong interaction which arise in certain limits, such as
204 the chiral or the heavy quark limit, to establish that nonperturbative effects are suppressed by small
205 parameters, and to estimate or extract them from data (e.g., measuring $|V_{us}|$ and $|V_{cb}|$, inclusive rates).
- 206 • Lattice QCD is a model-independent method to address nonperturbative phenomena. In practice, the
207 most precise results are for matrix elements involving at most one hadron in the initial and the final
208 state (allowing, e.g., extractions of magnitudes of CKM elements).

209 All of these approaches use experimental data from related processes to fix some parameters, constrain the
210 uncertainties, and cross-check the methods. Thus, experimental progress on a broad program will not only
211 reduce the uncertainties of key measurements, but also help reduce theoretical uncertainties.

212 As an example, consider extracting γ from $B \rightarrow DK$. This is one of the cleanest measurements in terms
213 of theoretical uncertainties, because all the necessary hadronic quantities can be measured. All $B \rightarrow DK$
214 based analyses consider decays of the type $B \rightarrow D^0(\bar{D}^0) K(X) \rightarrow F_D K(X)$, where F_D is a final state that

215 is accessible in both D^0 and \bar{D}^0 decay, allowing for interference, and X represents possible extra particles
 216 in the final state. Using several $B \rightarrow DKX$ decays modes (say, n different X states and k different D^0 and
 217 \bar{D}^0 decay modes), one can perform nk measurements, which depend on $n + k$ decay amplitudes. Thus, one
 218 can determine all hadronic parameters, as well as the weak phase γ , with very little theoretical uncertainty.

219 The main reason why many CP asymmetry measurements have small theoretical uncertainties is because
 220 they involve ratios of rates, from which the leading amplitudes cancel, so the uncertainties are suppressed by
 221 the relative magnitude of the subleading amplitudes. This is the case for the time dependent CP asymmetry
 222 in $B \rightarrow \psi K_S$, in which case the subdominant amplitude is suppressed by a factor ~ 50 due to CKM elements
 223 and by the ratio of the matrix element of a loop diagram compared to a tree diagram. However, it is not
 224 simple to precisely quantify the uncertainties below the percent level. In other modes (e.g., $B \rightarrow \phi K_S$, $\eta' K_S$,
 225 etc.) the loop suppression of the hadronic uncertainty is absent, and the theoretical understanding directly
 226 impacts at what level new physics can be unambiguously observed.

227 Symmetries of the strong interaction that occur for hadrons containing light quarks ($m_{u,d,s} < \Lambda_{\text{QCD}}$) or for
 228 hadrons containing a heavy quark ($m_{b,c} > \Lambda_{\text{QCD}}$) have played critical roles in understanding flavor physics.
 229 Chiral perturbation theory has been very important for kaon physics, and isospin symmetry is crucial for
 230 the determination of α in $B \rightarrow \pi\pi$, $\rho\rho$, and $\rho\pi$ decays. For B and D mesons, extra symmetries of the
 231 Lagrangian emerge in the $m_{b,c} \gg \Lambda_{\text{QCD}}$ limit, and these heavy quark spin-flavor symmetries imply, for
 232 example, that exclusive semileptonic $B \rightarrow D^{(*)}\ell\bar{\nu}$ decays are described by a single universal Isgur-Wise
 233 function in the symmetry limit. For inclusive semileptonic B decays, an operator product expansion can be
 234 used to compute sufficiently inclusive rates; applications include the extraction of $|V_{cb}|$. As is often the case,
 235 after understanding the symmetry limit and its implications, it is the analysis of subleading effects where
 236 many theoretical challenges lie. The theoretical tools to make further progress are well-developed, but much
 237 work remains to be done to reach the ultimate sensitivities.

238 Lattice QCD has become an important tool in flavor physics, and significant improvements are expected.
 239 As substantial investment in computational infrastructure is required, a separate section discusses it in this
 240 report. Lattice QCD allows first-principles calculations of some nonperturbative phenomena. In practice,
 241 approximations have to be made due to finite computing power, which introduce systematic uncertainties
 242 that can be studied (e.g., dependence on lattice spacing, spatial volume, etc.). Due to new algorithms and
 243 more powerful computers, matrix elements which contain at most one hadron in the final state should soon
 244 be calculable with percent level uncertainties. Matrix elements involving states with sizable widths, e.g., ρ
 245 and K^* , are more challenging. So are calculations of matrix elements containing more than one hadron in
 246 the final state, and it will require major developments to obtain small uncertainties for those. Thus, lattice
 247 QCD errors are expected to become especially small for leptonic and semileptonic decays, and meson mixing.

248 In summary, there are many observables with theoretical uncertainties at the few percent level, matching the
 249 expected experimental sensitivity, which is necessary to allow a discovery of small new physics contributions.
 250 The full exploitation of the experimental program requires continued support of theoretical developments.

251 1.3 Report of the Kaon Task Force

252 Kaon decays have played a pivotal role in shaping the standard model (SM). Prominent examples include
 253 the introduction of internal “flavor” quantum numbers (strangeness), parity violation ($K \rightarrow 2\pi$, 3π puzzle),
 254 quark mixing, meson-antimeson oscillations, discovery of CP violation, suppression of flavor-changing neutral
 255 currents (FCNC), discovery of the GIM (Glashow-Iliopoulos-Maiani) mechanism and prediction of charm.
 256 Now and looking ahead, kaons continue to have high impact in constraining the flavor sector of possible
 257 extensions of the SM.

Observable	SM Theory	Current Expt.	Future Experiments
$\mathcal{B}(K^+ \rightarrow \pi^+ \nu \bar{\nu})$	$7.81(75)(29) \times 10^{-11}$	$1.73_{-1.05}^{+1.15} \times 10^{-10}$ E787/E949	$\sim 10\%$ at NA62 $\sim 5\%$ at ORKA $\sim 2\%$ at Project-X
$\mathcal{B}(K_L^0 \rightarrow \pi^0 \nu \bar{\nu})$	$2.43(39)(6) \times 10^{-11}$	$< 2.6 \times 10^{-8}$ E391a	1 st observation at KOTO $\sim 5\%$ at Project-X
$\mathcal{B}(K_L^0 \rightarrow \pi^0 e^+ e^-)$	$(3.23_{-0.79}^{+0.91}) \times 10^{-11}$	$< 2.8 \times 10^{-10}$ KTeV	$\sim 10\%$ at Project-X
$\mathcal{B}(K_L^0 \rightarrow \pi^0 \mu^+ \mu^-)$	$(1.29_{-0.23}^{+0.24}) \times 10^{-11}$	$< 3.8 \times 10^{-10}$ KTeV	$\sim 10\%$ at Project-X
$ P_T $ in $K^+ \rightarrow \pi^0 \mu^+ \nu$	$\sim 10^{-7}$	< 0.0050	< 0.0003 at TREK < 0.0001 at Project-X
$\Gamma(K_{e2})/\Gamma(K_{\mu 2})$	$2.477(1) \times 10^{-5}$	$2.488(12) \times 10^{-5}$ (NA62, KLOE)	$\pm 0.0054 \times 10^{-5}$ at TREK $\pm 0.0025 \times 10^{-5}$ at Project-X
$\mathcal{B}(K_L^0 \rightarrow \mu^\pm e^\mp)$	$< 10^{-25}$	$< 4.7 \times 10^{-12}$	$< 2 \times 10^{-13}$ at Project-X

Table 1-2. A summary of the reach of current and proposed experiments for some key rare kaon decay measurements, in comparison to standard model theory and the current best experimental results. In the SM predictions for the $K \rightarrow \pi \nu \bar{\nu}$ and $K \rightarrow \pi \ell^+ \ell^-$ the first error is parametric, the second denotes the intrinsic theoretical uncertainty.

258 In the arena of kaon decays, a key role is played by the FCNC modes mediated by the quark-level processes
259 $s \rightarrow d(\gamma, \ell^+ \ell^-, \nu \bar{\nu})$, and in particular the four theoretically cleanest modes $K^+ \rightarrow \pi^+ \nu \bar{\nu}$, $K_L \rightarrow \pi^0 \nu \bar{\nu}$,
260 $K_L \rightarrow \pi^0 e^+ e^-$, $K_L \rightarrow \pi^0 \mu^+ \mu^-$. Because of the peculiar suppression of the SM amplitude (top-quark loop
261 suppressed by $|V_{td} V_{ts}| \sim \lambda^5$) which in general is not present in SM extensions, kaon FCNC modes offer a
262 unique window on the flavor structure of such extensions. This argument by itself provides a strong and
263 model-independent motivation to study these modes in the LHC era. Rare kaon decays can elucidate the
264 flavor structure of SM extensions, information that is in general not accessible from high-energy colliders.

265 The actual “discovery potential” depends on the precision of the prediction for these decays in the SM, the
266 level of constraints from other observables, and how well we can measure their branching ratios.

267 1.3.1 Rare kaon decays in the standard model: status and forecast

268 State-of-the-art predictions (see Ref. [16] and references therein) are summarized in Table 1-2 along with
269 current and expected experimental results. The predictions show our current knowledge of the theoretical
270 branching ratio uncertainties: $K^+ \rightarrow \pi^+ \nu \bar{\nu}$ at the 10% level, $K_L \rightarrow \pi^0 \nu \bar{\nu}$ at the 15% level, and $K_L \rightarrow \pi^0 e^+ e^-$
271 and $K_L \rightarrow \pi^0 \mu^+ \mu^-$ at the 25–30% level. In the neutrino modes, the irreducible theoretical uncertainty is
272 a small fraction of the total, which is currently dominated by the uncertainty in CKM parameters. In the
273 charged lepton modes, the uncertainty is dominated by long distance contributions which can be parametrized
274 in terms of the rates of other decays (such as $K_S \rightarrow \pi^0 \ell^+ \ell^-$). It is expected that in the next decade progress
275 in lattice QCD and in B meson measurements (LHCb and Belle II) will reduce the uncertainty on both
276 $K \rightarrow \pi \nu \bar{\nu}$ modes to the 5% level. Substantial improvements in $K_L \rightarrow \pi^0 \ell^+ \ell^-$ will have to rely on lattice
277 QCD computations, requiring evaluation of bi-local operators. Exploratory steps exist, but involve new
278 techniques, making it hard to forecast the level of uncertainty that can be achieved. Therefore, from a
279 theory perspective, the golden modes remain the $K \rightarrow \pi \nu \bar{\nu}$ decays, because they have small long-distance

contamination (negligible in the CP-violating K_L mode). The $K \rightarrow \pi\nu\bar{\nu}$ decay rates, especially in the K_L mode, can be predicted with smaller theoretical uncertainties than other FCNC decay rates involving quarks.

1.3.2 Beyond the standard model physics reach

The beyond the standard model (BSM) reach of rare FCNC kaon decays has received significant attention in the literature, through both explicit model analyses and model-independent approaches based on effective field theory (EFT). In the absence of a clear candidate for the TeV extension of the SM, the case for discovery potential and model-discriminating power can be presented very efficiently in terms of an EFT approach to BSM physics. In this approach, one parametrizes the effects of new heavy particles in terms of local operators whose coefficients are suppressed by inverse powers of the heavy new physics mass scale. The important point is that the EFT approach allows us to make statements that apply to classes of models, not just any specific SM extension. In this context, one can ask two important questions: (i) how large a deviation from the SM can we expect in rare decays from existing constraints? (ii) if a given class of operators dominates, what pattern of deviations from the SM can we expect in various rare kaon decays?

Our discussion here parallels the one given in Ref. [18], to which we refer for more details. To leading order in v/Λ (where $v \sim 200$ GeV and Λ is the scale of new physics), six operators can affect the $K \rightarrow \pi\nu\bar{\nu}$ decays. Three of these are four-fermion operators and affect the $K \rightarrow \pi\ell^+\ell^-$ decays as well (one of these operators contributes to $K \rightarrow \pi\ell\nu$ by $SU(2)$ gauge invariance). The coefficients of these operators are largely unconstrained by other observables, and therefore one can expect sizable deviations from the SM in $K \rightarrow \pi\nu\bar{\nu}$ (both modes) and $K \rightarrow \pi\ell^+\ell^-$, depending on the flavor structure of the BSM scenario.

The other three leading operators contributing to $K \rightarrow \pi\nu\bar{\nu}$ involve the Higgs field and reduce, after electroweak symmetry breaking, to effective flavor-changing Z -boson interactions, with both left-handed (LH) and right-handed (RH) couplings to quarks. These “ Z -penguin” operators (both LH and RH) are the leading effect in many SM extensions, and affect a large number of kaon observables ($K \rightarrow \pi\ell^+\ell^-$, ϵ_K , ϵ'_K/ϵ_K , and in the case of one operator $K \rightarrow \pi\ell\nu$ through $SU(2)$ gauge invariance). Focusing on this class of operators, the relevant part of the effective Lagrangian reads

$$\mathcal{L}_{\text{eff}} \propto (\lambda_t C_{\text{SM}} + C_{\text{NP}}) \bar{d}_L \gamma_\mu s_L Z^\mu + \tilde{C}_{\text{NP}} d_R \gamma_\mu s_R Z^\mu, \quad (1.2)$$

where $\lambda_q = V_{qs}^* V_{qd}$ with V_{ij} denoting elements of the CKM matrix, and $C_{\text{SM}} \approx 0.8$ encodes the SM contribution to the LH Z -penguin (the RH Z -penguin is highly suppressed in the SM by small quark masses). Assuming dominance of the Z -penguin operators, one can study the expectations for the $K \rightarrow \pi\nu\bar{\nu}$ branching ratio for different choices of the effective couplings C_{NP} , \tilde{C}_{NP} , and address the correlations with other observables. This is illustrated in Fig. 1-2. In this framework, ϵ'_K/ϵ_K provides the strongest constraint on the CP violating mode $K_L \rightarrow \pi^0\nu\bar{\nu}$ [19, 20, 21, 22, 23]. This is illustrated by the green bands in Fig. 1-2, where one can see that the requirement $\epsilon'_K/\epsilon_K \in [0.2, 5](\epsilon'_K/\epsilon_K)_{\text{exp}}$ limits deviations in the $K_L \rightarrow \pi^0\nu\bar{\nu}$ to be of $\mathcal{O}(1)$, while leaving room for larger deviations in the CP conserving mode $K^+ \rightarrow \pi^+\nu\bar{\nu}$. The correlation between ϵ'_K/ϵ_K and $K_L \rightarrow \pi^0\nu\bar{\nu}$ can be evaded only if there is a cancellation among the Z -penguin and other contributions to ϵ'_K/ϵ_K . Moreover, we stress that this conclusion holds in all models in which the Z -penguin provides the dominant contribution to $K \rightarrow \pi\nu\bar{\nu}$ decays. While this is not true in general, we think this constraint should be one of the drivers of the design sensitivity for $K_L \rightarrow \pi^0\nu\bar{\nu}$ experiments.

The number of operators that affect the $K_L \rightarrow \pi^0\ell^+\ell^-$ ($\ell = e, \mu$) decays is larger than the case of $K \rightarrow \pi\nu\bar{\nu}$. Besides (axial-)vector operators resulting from Z - and photon-penguin diagrams, (pseudo-)scalar operators associated with Higgs exchange can play a role [28]. In a model-independent framework:

$$\mathcal{L}_{\text{eff}} \supset C_A Q_A + C_V Q_V + C_P Q_P + C_S Q_S, \quad (1.3)$$

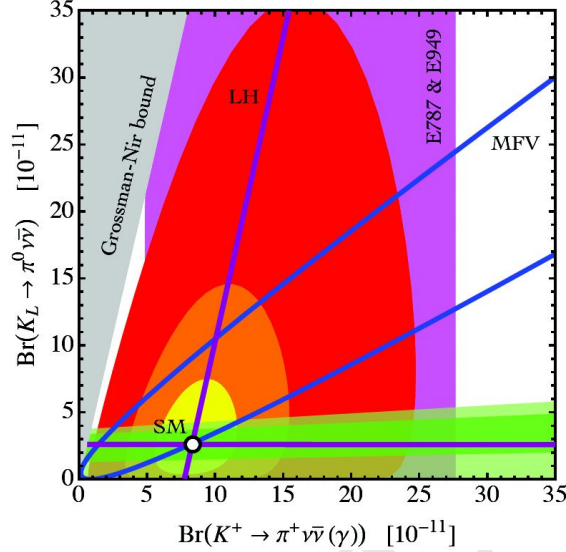


Figure 1-2. Predictions for the $K \rightarrow \pi \nu \bar{\nu}$ branching ratios assuming dominance of the Z -penguin operators, for different choices of the effective couplings $C_{\text{NP}}, \tilde{C}_{\text{NP}}$ [24]. The SM point is indicated by a white dot with black border. The yellow, orange, and red shaded contours correspond to $|C_{\text{NP}}, \tilde{C}_{\text{NP}}| \leq \{0.5, 1, 2\} |\lambda_t C_{\text{SM}}|$, the magenta band indicates the 68% confidence level (CL) constraint on $\mathcal{B}(K^+ \rightarrow \pi^+ \nu \bar{\nu} (\gamma))$ from experiment [25], and the gray area is theoretically inaccessible [26]. The blue parabola represents the subspace accessible to MFV models. The purple straight lines represent the subspace accessible in models that have only LH currents, due to the constraint from ϵ_K [27]. The green band represents the region accessible after taking into account the correlation of $K_L \rightarrow \pi^0 \nu \bar{\nu}$ with ϵ'_K/ϵ_K : the (light) dark band corresponds to predictions of ϵ'_K/ϵ_K within a factor of (5) 2 of the experimental value, using central values for the hadronic matrix elements as reported in [20] and references therein.

320 with

$$Q_A = (\bar{d}\gamma^\mu s)(\bar{\ell}\gamma_\mu\gamma_5\ell), \quad Q_V = (\bar{d}\gamma^\mu s)(\bar{\ell}\gamma_\mu\ell), \quad Q_P = (\bar{d}s)(\bar{\ell}\gamma_5\ell), \quad Q_S = (\bar{d}s)(\bar{\ell}\ell). \quad (1.4)$$

321 In Figure 1-3 we depict the accessible parameter space corresponding to various classes of NP. The blue
 322 parabola illustrates again the predictions obtained by allowing only for a contribution C_{NP} with arbitrary
 323 modulus and phase. We see that in models with dominance of the LH Z -penguin the deviations in $K_L \rightarrow$
 324 $\pi^0 \ell^+ \ell^-$ are strongly correlated. A large photon-penguin can induce significant corrections in C_V , which
 325 breaks this correlation and opens up the parameter space as illustrated by the dashed orange parabola and
 326 the yellow shaded region. The former predictions are obtained by employing a common rescaling of $C_{A,V}$,
 327 while in the latter case the coefficients $C_{A,V}$ are allowed to take arbitrary values. If besides $Q_{A,V}$ also
 328 $Q_{P,S}$ can receive sizable NP corrections a further relative enhancement of $\text{Br}(K_L \rightarrow \pi^0 \mu^+ \mu^-)$ compared to
 329 $\text{Br}(K_L \rightarrow \pi^0 e^+ e^-)$ is possible. This feature is exemplified by the light blue shaded region that corresponds
 330 to the parameter space that is compatible with the constraints on $C_{P,S}$ arising from $K_L \rightarrow \mu^+ \mu^-$. Finally,
 331 we note that $K_L \rightarrow \mu^+ \mu^-$ itself is another FCNC mode of interest, as it is sensitive to different combinations
 332 of new physics couplings. The constraining power of $K_L \rightarrow \mu^+ \mu^-$ is limited by the current understanding of
 333 the dispersive part of the amplitude. Despite this, the mode already provides useful diagnostic power, as in
 334 combination with $K \rightarrow \pi \nu \bar{\nu}$ can help distinguish among LH or RH coupling of Z and Z' to quarks [29, 30, 31].

335 Rare kaon decays have been extensively studied within well motivated extensions of the SM, such as
 336 supersymmetry (SUSY) [32] and warped extra dimensions (Randall-Sundrum) models [20, 29]. In all cases,
 337 deviations from the SM can be sizable and perhaps most importantly the correlations between various rare
 338 K decays are essential in discriminating among models. Rare $K \rightarrow \pi \nu \bar{\nu}$ experiments can also probe the

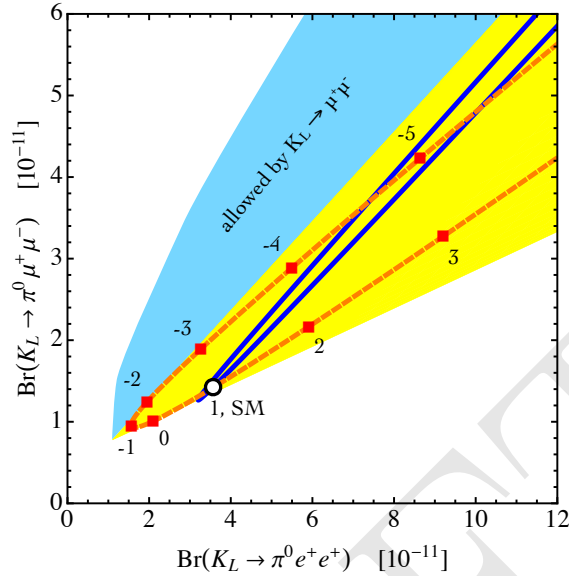


Figure 1-3. Predictions for the $K_L \rightarrow \pi^0 \ell^+ \ell^-$ branching ratios assuming different types of NP contributions [24]. The SM point is indicated by a white dot with black border. The blue parabola represents the region accessible by allowing only for C_{NP} with arbitrary modulus and phase. The subspace accessible when $C_{V,A} \neq 0$ is represented by the dashed orange parabola (common rescaling of $C_{A,V}$) and the yellow shaded region (arbitrary values of $C_{A,V}$). The subspace accessible when $C_{S,P} \neq 0$ (compatibly with $K_L \rightarrow \mu^+ \mu^-$) is represented by the light blue shaded region.

339 existence of light states very weakly coupled to the SM appearing in various dark sector models [33], through
 340 the experimental signature $K \rightarrow \pi +$ (missing energy), and distortions to the pion spectrum.

341 Other modes

342 Besides the FCNC modes, kaon decays also provide exquisite probes of the charged-current sector of SM
 343 extensions, probing scales of TeV or above. Theoretically, the cleanest probes are (i) the ratio $R_K \equiv$
 344 $\Gamma(K \rightarrow e\nu)/\Gamma(K \rightarrow \mu\nu)$, which tests lepton universality, scalar, and tensor charged-current interactions;
 345 (ii) the transverse muon polarization P_μ^T in the semi-leptonic decay $K^+ \rightarrow \pi^0 \mu^+ \nu_\mu$, which is sensitive to
 346 BSM sources of CP violation in scalar charged-current operators. In both cases there is a clean discovery
 347 window provided by the precise SM theoretical prediction [34] (R_K) and by the fact that in the SM P_μ^T is
 348 generated only by very small and known final state interactions [35]. Table 1-2 provides a summary of SM
 349 predictions for these processes, along with current and projected experimental sensitivities at ongoing or
 350 planned experiments.

351 1.3.3 Experimental program

352 Following the termination of a world-class kaon program in the U.S. by 2002, leadership in kaon physics
 353 shifted to Europe and Japan, where a program of experiments aiming for orders of magnitude improvements
 354 in reach for new physics is now in progress.

355 The NA62 experiment at CERN [36] uses a novel in-flight technique to search for $K^+ \rightarrow \pi^+ \nu \bar{\nu}$ and will finish
 356 commissioning at the end of 2013 and start physics running toward the end of 2014. The NA62 goal is to
 357 measure the $K^+ \rightarrow \pi^+ \nu \bar{\nu}$ branching ratio with 10% precision along with a robust and diverse kaon physics
 358 program.

359 The KOTO experiment at JPARC [37] is an in-flight measurement of $K_L^0 \rightarrow \pi^0 \nu \bar{\nu}$. Significant experience
 360 and a better understanding of the backgrounds were obtained in its predecessor, E391a. The anticipated
 361 experimental sensitivity is a few SM signal events in three years of running with 300 kW of beam power.
 362 Commissioning runs were undertaken in 2012 and 2013 and physics running started in 2013, but the longer
 363 term performance of the experiment will depend upon beam power evolution of the JPARC accelerator.

364 The TREK experiment at JPARC [38] will search for T violation in stopped charged kaon decays by
 365 measuring the polarization asymmetry in $K^+ \rightarrow \pi^0 \mu^+ \nu_\mu$ decays. TREK needs at least 100 kW (the proposal
 366 assumed 270 kW) for this measurement. While the accelerator is running at lower power, collaborators have
 367 proposed a search for lepton flavor universality violation through the measurement of $\Gamma(K \rightarrow e \nu)/\Gamma(K \rightarrow \mu \nu)$
 368 at the 0.2% level, which will use much of the TREK apparatus and requires only 30 kW of beam power
 369 and will be ready to run in 2015. At the same time, this configuration allows for sensitive searches for
 370 a heavy sterile neutrino (N) in $K^+ \rightarrow \mu^+ N$, and for light bosons (heavy photons from the dark sector,
 371 $A' \rightarrow e^+ e^-$) in the $K^+ \rightarrow \mu^+ \nu_\mu e^+ e^-$ and $K^+ \rightarrow \pi^+ e^+ e^-$ decays, where the new particles would be
 372 identified as narrow peaks in the respective momentum and $e^+ e^-$ invariant mass spectra. The uncertainty
 373 of the JPARC beam power profile and potential conflicts for beamline real estate make the long term future
 374 of the TREK experiment unclear.

375 The KLOE-2 experiment [39] will extend the results of KLOE to improve neutral kaon interference measure-
 376 ments, CPT and quantum mechanics tests and a wide range of measurements of non-leptonic and radiative
 377 kaon decays.

378 The ORKA experiment is proposed to measure $K^+ \rightarrow \pi^+ \nu \bar{\nu}$ with 1000 event sensitivity at the Fermilab
 379 Main Injector (MI) [40]. After a five year run ORKA will reach a precision of 5% on the branching ratio,
 380 which is the expected level of theoretical precision. This high-precision measurement would be one of the
 381 most incisive probes of quark flavor physics in the coming decade. ORKA is a stopped kaon experiment that
 382 builds on the experience of the E787/949 experiments at Brookhaven that observed seven candidate events.
 383 Backgrounds, primarily from other kaon decays at branching fractions as much as 10 orders of magnitude
 384 larger, have similar signatures to the signal. ORKA takes advantage of the extensive knowledge of background
 385 rates and characteristics from E787/E949 by using the same proven experimental techniques. The methods
 386 for suppressing backgrounds are well known, as are the background rates and experimental acceptance.
 387 Improvements in detector performance are possible due to significant advances in detector technology in the
 388 25 years since E787 first ran. The new ORKA detector with beam supplied by the MI running at 95 GeV with
 389 moderate duty factor presents an opportunity to extend the E787/E949 approach by two orders of magnitude
 390 in sensitivity. The first order of magnitude improvement comes from the substantially brighter source of
 391 low energy kaons and the second arises from incremental improvements to the experimental techniques
 392 firmly established at BNL. ORKA will observe 210 SM events per year and will make a wide variety of
 393 measurements in addition to the $K^+ \rightarrow \pi^+ \nu \bar{\nu}$ mode. ORKA will search for and study a range of important
 394 reactions involving kaon and pion decays, such as tests of lepton universality, symmetry violations, hidden
 395 sector particles, heavy neutrinos and other topics. ORKA will be a world-leading kaon physics experiment,
 396 train a new generation of kaon physicists and position the U.S. to move forward to a Project-X kaon program.
 397 It is an essential step in developing a robust intensity frontier program in the U.S. at Project-X.

398 The U.S. has an opportunity through ORKA to re-establish a leadership position in kaon physics.

Project-X

A flagship experiment of the Project-X physics program will measure the $K_L^0 \rightarrow \pi^0 \nu \bar{\nu}$ branching ratio with 5% precision. This effort will build on the KOTO experience, benefit from the KOPIO initiative [41] and take advantage of the beam power and flexibility provided by Stage 2 of Project-X.

KOPIO proposed to measure $K_L^0 \rightarrow \pi^0 \nu \bar{\nu}$ with a SM sensitivity of 100 events at the BNL Alternating Gradient Synchrotron (AGS) as part of the RSVP (Rare Symmetry Violating Processes) project. The experimental technique and sensitivity were well-developed and extensively reviewed. KOPIO was designed to use a neutral beam at a 42° targeting angle produced by 24 GeV protons from the AGS. The neutral kaons would have an average momentum of 800 MeV/c with a range of 300–1500 MeV/c. A low momentum beam was critical for the Time-Of-Flight (TOF) strategy of the experiment.

The TOF technique is even better matched to the kaon momentum produced by the 3 GeV proton beam at Project-X where the higher momentum tail present in the AGS beam is suppressed. Performance of the TOF strategy was limited by the design bunch width of 200 ps at the AGS. The Project-X beam pulse timing, including target time slewing, is expected to be less than 50 ps and would substantially improve the momentum resolution and background rejection capability of the $K_L^0 \rightarrow \pi^0 \nu \bar{\nu}$ experiment driven with the Project-X beam.

The AGS K_L yield per proton is 20 times the Project-X yield; however, the 0.5 mA Project-X proton flux is 150 times the RSVP goal of 10^{14} protons every 5 seconds. Hence the neutral kaon flux at Project-X will be 8 times the AGS flux goal into the same beam acceptance. The Project-X neutral beam will contain about a factor of three more neutrons, but neutron interactions will be highly suppressed by the evacuated beamline and detector volume. The nominal five-year Project-X run is 2.5 times longer than the KOPIO initiative at the AGS and hence the reach of a Project-X $K_L^0 \rightarrow \pi^0 \nu \bar{\nu}$ experiment would be 20 times greater than RSVP.

A TOF-based $K_L^0 \rightarrow \pi^0 \nu \bar{\nu}$ experiment driven by Project-X would be re-optimized for the Project-X K_L momentum spectrum, TOF resolution and corresponding background rejection. It is likely that this optimization would result in a smaller neutral beam solid angle which would simplify the detector design, increase the acceptance and relax the requirement to tag photons in the fierce rate environment of the neutral beam. Optimizing the performance will probably require a proton pulse train frequency of 20–50 MHz and an individual proton pulse timing width of ~ 20 ps. Based on the E391a and KOTO experience, a careful design of the target and neutral beam channel is required to minimize the neutron halo and to assure target survival in the intense proton beam. The high K_L beam flux and the potential of break-through improvements in TOF performance and calorimeter technology support the viability of a $K_L^0 \rightarrow \pi^0 \nu \bar{\nu}$ experiment with ~ 1000 SM event sensitivity.

If ORKA [40] observes a significant non-SM result, the $K^+ \rightarrow \pi^+ \nu \bar{\nu}$ decay mode could be studied with higher statistics with a K^+ beam driven by Project-X. The high-purity, low-momentum K^+ beam designed for ORKA could also serve experiments to precisely measure the polarization asymmetry in $K^+ \rightarrow \pi^0 \mu^+ \nu_\mu$ decays and to continue the search for lepton flavor universality violation through the measurement of $\Gamma(K \rightarrow e\nu)/\Gamma(K \rightarrow \mu\nu)$ at high precision.

Depending upon the outcome of the TREK experiment at JPARC, a T violation experiment would be an excellent candidate for Project-X, as would a multi-purpose experiment dedicated to rare modes that involve both charged and neutral particles in the final state. This experiment might be able to pursue $K_L \rightarrow \pi^0 \ell^+ \ell^-$ as well as many other radiative and leptonic modes. The kaon physics program at Project-X could be very rich indeed.

1.3.4 Conclusions

Kaon decays are extremely sensitive probes of the flavor and CP-violating sector of any SM extension. The $K \rightarrow \pi\nu\bar{\nu}$ golden modes have great discovery potential: (i) sizable, $\mathcal{O}(1)$, deviations from the SM are possible; (ii) even small deviations can be detected due to the precise theoretical predictions. Next generation searches should aim for a sensitivity level of 10^3 SM events (few % uncertainty) in both K^+ and K_L modes, in order to maximize discovery potential.

We foresee searches for both $K \rightarrow \pi\nu\bar{\nu}$ modes as flagship measurements of a reinigorated US-led kaon program. As summarized in Table 1-2, through ORKA and Project-X this program has the opportunity to pursue a broad set of measurements, exploring the full discovery potential and model-discrimination power of kaon physics.

1.4 Report of the B -Physics Task Force

1.4.1 Physics Motivation: searches for BSM physics

Rare B physics processes are sensitive to new physics (NP) because the heavy particles can contribute through virtual corrections to the effective weak Hamiltonian. In this way one can, e.g., probe extended Higgs sectors, test for the presence of new gauge interactions or for extended matter content such as the ones encountered in supersymmetric models. The sensitivity to NP depends on how large the flavor violating couplings are. For instance, in the most conservative case of Minimal Flavor Violation (MFV) with new particles only contributing in the loops, the rare B processes can probe mass scales of roughly $\sim \mathcal{O}(\text{TeV})$ with the next generation experiments. In the case of general flavor violation with $\mathcal{O}(1)$ off-diagonal couplings, on the other hand, one probes mass scales of $\mathcal{O}(10^3 \text{ TeV})$ [1]. Because the dependence on new particle masses and (flavor violating) couplings is different than in the on-shell production, the NP searches at LHCb and Belle II are also complementary to the high p_T NP searches at ATLAS and CMS.

Observables that are especially interesting for the future B physics program are those that have small or systematically improvable theoretical uncertainties. An important input is provided by measurements of the standard CKM unitarity triangle. The angle γ and modulus $|V_{ub}|$ are determined from tree-level processes and thus less prone to contributions from NP. They provide the SM “reference” determination of the CKM unitarity triangle (in effect its apex, the values of $\bar{\rho}$ and $\bar{\eta}$). $|V_{ub}|$ is measured from inclusive and exclusive $b \rightarrow u\ell\nu$ processes. There is an on-going effort to improve the theory predictions using both the continuum methods and lattice QCD, and a factor of a few improvements on the errors seem feasible. For instance, the present theory error on $|V_{ub}|$ from exclusive $B \rightarrow \pi\ell\nu$ can be reduced from present 8.7% to 2% by 2018 [42] (see Table 1-6). The theoretical uncertainties in the measurement of γ from $B \rightarrow DK$ decays are even smaller. All the required hadronic matrix elements can be measured, because of the cascade nature of the $B \rightarrow DK$, $D \rightarrow f$ decay, if enough final states f are taken into account. The irreducible theoretical errors thus enter only at the level of one-loop electroweak corrections and are below $\mathcal{O}(10^{-6})$ [43]. The present experimental errors are $\pm 12^\circ$ from the average of BABAR and Belle measurements. LHCb has recently matched this precision. The errors are statistics-limited and will be substantially decreased in the future.

The tree-level determinations of $\bar{\rho}$ and $\bar{\eta}$ can then be compared with the measurements from loop-induced FCNCs, for instance with the time-dependent CP asymmetry in $B \rightarrow J/\psi K_S$ and related modes determining the angle β . With improved theoretical control BSM physics can be constrained or even discovered. NP could also enter in the $B_s - \bar{B}_s$ mixing. In the SM the mixing phase is small, suppressed by λ^2 compared to β .

481 Thus, in the SM, the corresponding time-dependent CP asymmetry in the $b \rightarrow c\bar{c}s$ dominated decays, such as
 482 $B_s \rightarrow J/\psi \phi$, is predicted very precisely, $\beta_s^{(\text{SM})} = 0.0182 \pm 0.0008$. The LHCb result, $\beta_s = -0.035 \pm 0.045$ [44],
 483 is consistent with the SM expectation, but the statistical uncertainty is much greater than that of the SM
 484 prediction. Since the uncertainty of the SM prediction is very small, future significant improvements of the
 485 measurement of β_s will directly translate to a better sensitivity to BSM physics.

486 Another important search for NP is to compare the time-dependent CP asymmetries of penguin-dominated
 487 $b \rightarrow q\bar{q}s$ processes with the tree dominated $b \rightarrow c\bar{c}s$ decays. Observables that probe this are the differences
 488 of CP asymmetries $S_{J/\psi K_S} - S_{\phi K_S}$, $S_{\psi K_S} - S_{\eta' K_S}$, etc., in B_d decay, and $S_{J/\psi \phi} - S_{\phi \phi}$ in B_s decay.

489 The list of interesting observables in *B* physics is very long. One could emphasize in particular the rare *B*
 490 decays with leptons in the final state. The $B_s \rightarrow \ell^+ \ell^-$ decay is especially interesting for SUSY searches
 491 in view of the fact that these are $(\tan \beta)^6$ enhanced. LHCb presented first evidence of this decay, with
 492 $\mathcal{B}(B_s \rightarrow \mu^+ \mu^-) = (3.2_{-1.2}^{+1.5}) \times 10^{-9}$ [45] consistent with the SM prediction $(3.54 \pm 0.30) \times 10^{-9}$ [46, 47]. Also,
 493 CMS has very recently reported a measurement of $\mathcal{B}(B_s \rightarrow \mu^+ \mu^-) = (3.0_{-0.9}^{+1.0}) \times 10^{-9}$ [48] consistent with
 494 the earlier LHCb result, and LHCb has also updated its value to $\mathcal{B}(B_s \rightarrow \mu^+ \mu^-) = (2.9_{-1.0}^{+1.1}) \times 10^{-9}$ [49].
 495 This puts strong constraints on the large $\tan \beta$ region of MSSM, favored by the measured Higgs mass for the
 496 case of TeV scale squarks. The theoretical errors on the SM prediction are still several times smaller than
 497 the experimental ones, making more precise measurements highly interesting. With the LHCb upgrade, the
 498 search for $B_d \rightarrow \ell^+ \ell^-$ will also get near the SM level. Rare decays involving a $\nu\bar{\nu}$ pair are theoretically
 499 very clean, and Belle II should reach the SM level in $B \rightarrow K^{(*)} \nu\bar{\nu}$; the current constraints are an order of
 500 magnitude weaker. There is also a long list of interesting measurements in $b \rightarrow s\gamma$ and $b \rightarrow s\ell^+ \ell^-$ mediated
 501 inclusive and exclusive decays, CP asymmetries, angular distributions, triple product correlations, etc., which
 502 will be probed much better in the future. The $s \leftrightarrow d$ processes, with lower SM rates, will provide many
 503 other challenging measurements and opportunities to find NP. Rare *B* decays can also be used as probes for
 504 “hidden sector” particle searches, for lepton flavor violation, and for baryon number violating processes.

505 There are also some intriguing deviations from the SM in the current data. The D0 collaboration measured
 506 the CP-violating dilepton asymmetry to be 4σ away from zero, $A_{\text{SL}}^b = (7.87 \pm 1.96) \times 10^{-3} \approx 0.6 A_{\text{SL}}^d +$
 507 $0.4 A_{\text{SL}}^s$ [50]. The measured semileptonic asymmetry is a mixture of B_d and B_s ones, where $A_{\text{SL}} \simeq 2(1 - |q/p|)$
 508 in each case measures the mismatch of the CP and mass eigenstates. The quantity $(1 - |q/p|)$ is model-
 509 independently suppressed by m_b^2/m_W^2 , with an additional m_c^2/m_b^2 suppression in the SM, which NP may
 510 violate [51]. Since the D0 result allows plenty of room for NP, it will be important for LHCb and Belle II to
 511 clarify the situation. LHCb has recently measured $A_{\text{SL}}^s = (-2.4 \pm 5.4 \pm 3.3) \times 10^{-3}$ [52] which complements
 512 A_{SL}^d measured at e^+e^- *B* factories. Further improvement in experimental errors on both quantities is needed.

513 Another interesting anomaly is the hint of the flavor universality violation in $B \rightarrow D^{(*)} \tau \nu$ decays observed
 514 by BABAR [53] which differ from the SM prediction expected from the $B \rightarrow D^{(*)} \ell \nu$ rates by 3.4σ . Combined
 515 with the slight excess of $\mathcal{B}(B \rightarrow \tau \nu)$ over the SM the measurements can be explained using charged Higgs
 516 exchange, e.g., in the two Higgs doublet model, but with nontrivial flavor structure [54]. The MFV hypothesis
 517 is not preferred. To settle the case it will require larger data sets at the future e^+e^- *B* factories (and
 518 measuring the $B \rightarrow \mu\bar{\nu}$ mode as well).

519 Any of the above measurements could lead to a discovery of new physics. In addition, a real strength of the
 520 *B* physics program is that a pattern of modifications in different measurements can help to zoom in on the
 521 correct NP model. Further information will also be provided by rare kaon decay experiments and searches
 522 for lepton flavor violation in charged lepton decays such as $\mu \rightarrow e\gamma$, μ -to- e conversion on a nucleus, $\tau \rightarrow \mu\gamma$,
 523 and $\tau \rightarrow 3\mu$. This program will provide complementary information to the on-shell searches at the LHC.

524 1.4.2 Physics potential of e^+e^- experiments: Belle II

525 The spectacular successes of the B -factory experiments Belle and BABAR highlight the advantages of e^+e^-
526 collider experiments:

- 527 • Running on the $\Upsilon(4S)$ resonance produces an especially clean sample of $B^0\bar{B}^0$ pairs in a quantum
528 correlated 1^{--} state. The low background level allows reconstruction of final states containing γ 's
529 and particles decaying to γ 's: π^0 , ρ^\pm , η , η' , etc. Neutral K_L^0 mesons are also efficiently reconstructed.
530 Detection of the decay products of one B allows the flavor of the other B to be tagged.
- 531 • Due to low track multiplicities and detector occupancy, the reconstruction efficiency is high and the
532 trigger bias is low. This substantially reduces corrections and systematic uncertainties in many types
533 of measurements, e.g., Dalitz plot analyses.
- 534 • By utilizing asymmetric beam energies, the Lorentz boost β of the e^+e^- system can be made large
535 enough such that a B or D meson travels an appreciable distance before decaying. This allows precision
536 measurements of lifetimes, mixing parameters, and CP violation (CPV). Note that measurement of the
537 D lifetime provides a measurement of the mixing parameter y_{CP} , while measurement of the B lifetime
538 (which is already well measured) allows one to determine the decay time resolution function from data.
- 539 • Since the absolute delivered luminosity is measured with Bhabha scattering, an e^+e^- experiment
540 measures *absolute* branching fractions. These are complementary to *relative* branching fractions
541 measured at hadron colliders, and in fact are used to normalize the relative measurements.
- 542 • Since the initial state is completely known, one can perform “missing mass” analyses, i.e., infer the
543 existence of new particles via energy/momentum conservation rather than reconstructing their final
544 states. By fully reconstructing a B decay in one hemisphere of the detector, inclusive decays such as
545 $B \rightarrow X_s \ell^+ \ell^-$, $X_s \gamma$ can be measured in the “opposite” hemisphere.
- 546 • In addition to producing large samples of B and D decays, an e^+e^- machine produces large sample
547 of τ leptons. This allows one to measure rare τ decays and search for forbidden τ decays with a high
548 level of background rejection.

549 To extend this physics program beyond the Belle and BABAR experiments, the KEKB e^+e^- accelerator
550 at the KEK laboratory in Japan will be upgraded to “SuperKEKB,” and the Belle experiment will be
551 upgraded to “Belle II.” The KEKB accelerator achieved a peak luminosity of $2.1 \times 10^{34} \text{ cm}^{-2}\text{s}^{-1}$, and the
552 Belle experiment recorded a total integrated luminosity of 1040 fb^{-1} (just over 1.0 ab^{-1}). The SuperKEKB
553 accelerator plans to achieve a luminosity of $8 \times 10^{35} \text{ cm}^{-2}\text{s}^{-1}$, and the Belle II experiment plans to record
554 50 ab^{-1} of data by 2022. As $\sigma(e^+e^- \rightarrow b\bar{b}) \approx 1.1 \text{ nb}$ at the $\Upsilon(4S)$ resonance, this data sample will contain
555 $5 \times 10^{10} B\bar{B}$ pairs. Such a large sample will improve the precision of time-dependent CPV measurements
556 and the sensitivity of searches for rare and forbidden decays. Systematic errors should also be reduced, as
557 control samples from which many are calculated will substantially increase.

558 A discussion of the complete physics program of Belle II is beyond the scope of this summary. Here we
559 touch upon only a few highlights. More complete writeups can be found in Refs. [55] and [56]; the latter
560 was written in the context of the proposed — but declined — SuperB experiment in Italy. The expected
561 sensitivity of Belle II in 50 fb^{-1} of data for various topical B decays is listed in Table 1-3.

562 As mentioned above, a main strength of a B factory experiment is the ability to make precision measurements
563 of CP violation, and this capability will be exploited to search for NP sources of CPV. The difference between
564 B^0 and \bar{B}^0 decay rates to a common self-conjugate state is sensitive to both direct CPV (i.e., occurring in
565 the B^0 and \bar{B}^0 decay amplitudes), and indirect CPV from interference between the $B \rightarrow f$ decay and
566 $B \rightarrow \bar{B}^0 \rightarrow f$ mixing amplitudes. The indirect CPV was originally measured at Belle and BABAR for

Observable	SM theory	Current measurement (early 2013)	Belle II (50 ab^{-1})
$S(B \rightarrow \phi K^0)$	0.68	0.56 ± 0.17	± 0.03
$S(B \rightarrow \eta' K^0)$	0.68	0.59 ± 0.07	± 0.02
α from $B \rightarrow \pi\pi, \rho\rho$		$\pm 5.4^\circ$	$\pm 1.5^\circ$
γ from $B \rightarrow DK$		$\pm 11^\circ$	$\pm 1.5^\circ$
$S(B \rightarrow K_S \pi^0 \gamma)$	< 0.05	-0.15 ± 0.20	± 0.03
$S(B \rightarrow \rho \gamma)$	< 0.05	-0.83 ± 0.65	± 0.15
$A_{\text{CP}}(B \rightarrow X_{s+d} \gamma)$	< 0.005	0.06 ± 0.06	± 0.02
A_{SL}^d	-5×10^{-4}	-0.0049 ± 0.0038	± 0.001
$\mathcal{B}(B \rightarrow \tau \nu)$	1.1×10^{-4}	$(1.64 \pm 0.34) \times 10^{-4}$	$\pm 0.05 \times 10^{-4}$
$\mathcal{B}(B \rightarrow \mu \nu)$	4.7×10^{-7}	$< 1.0 \times 10^{-6}$	$\pm 0.2 \times 10^{-7}$
$\mathcal{B}(B \rightarrow X_s \gamma)$	3.15×10^{-4}	$(3.55 \pm 0.26) \times 10^{-4}$	$\pm 0.13 \times 10^{-4}$
$\mathcal{B}(B \rightarrow X_s \ell^+ \ell^-)$	1.6×10^{-6}	$(3.66 \pm 0.77) \times 10^{-6}$	$\pm 0.10 \times 10^{-6}$
$\mathcal{B}(B \rightarrow K \nu \bar{\nu})$	3.6×10^{-6}	$< 1.3 \times 10^{-5}$	$\pm 1.0 \times 10^{-6}$
$A_{\text{FB}}(B \rightarrow K^* \ell^+ \ell^-)_{q^2 < 4.3 \text{ GeV}^2}$	-0.09	0.27 ± 0.14	± 0.04
$A_{\text{FB}}(B^0 \rightarrow K^{*0} \ell^+ \ell^-)$ zero crossing	0.16	0.029	0.008
$ V_{ub} $ from $B \rightarrow \pi \ell^+ \nu$ ($q^2 > 16 \text{ GeV}^2$)	9% \rightarrow 2%	11%	2.1%

Table 1-3. The expected reach of Belle II in 50 ab^{-1} of data for various topical B decay measurements. For comparison, also listed are the standard model expectation and the current best experimental results. For $|V_{ub}|$ we list the fractional error.

all-charged final states such as $J/\psi K^0$ [57, 58] (see Fig. 1-4, left) and $\pi^+ \pi^-$ [59, 60]; at Belle II, this measurement will be extended with good statistics to more challenging final states such as $B^0 \rightarrow K_S^0 K_S^0$ (Fig. 1-4, left, shows a first measurement by Belle), $B^0 \rightarrow K^0 \pi^0$, and $B^0 \rightarrow X_{s+d} \gamma$. The last mode proceeds via electromagnetic $b \rightarrow s \gamma$ and $b \rightarrow d \gamma$ penguin amplitudes, where X_{s+d} represents the hadronic system in these decays. In a fully inclusive measurement, the γ is measured but X_{s+d} is not reconstructed. In the SM there is a robust expectation that direct CP violation is negligible, i.e., the decay rates for B and \bar{B} to $X_{s+d} \gamma$ are equal. A measured difference would be a strong indication of NP, and differences of up to 10% appear in some non-SM scenarios. The best measurement with existing B -factory data is consistent with no difference and has a 7% absolute error [61]. Belle II should reduce this uncertainty to below 1%.

Both Belle and *BABAR* used the $b \rightarrow c \bar{c} s$ “tree” mode $B^0 \rightarrow J/\psi K^0$ to measure the phase β of the CKM unitary triangle to high precision: $\sin(2\beta) = 0.665 \pm 0.022$ [62]. However, this phase can also be measured in $b \rightarrow s \bar{s} s$ “loop” decays such as $B^0 \rightarrow \phi K^0$ and $B^0 \rightarrow \eta' K^0$. Since virtual NP contributions could compete with the SM loop diagrams, these modes are sensitive to NP. Comparing the values of $\sin(2\beta)$ measured in $b \rightarrow c \bar{c} s$ and in $b \rightarrow s \bar{s} s$ processes thus provides a way to search for NP. The decay $B^0 \rightarrow \eta' K^0$ is the most precisely measured $b \rightarrow s \bar{s} s$ mode; the value of $\sin(2\beta)$ obtained is 0.59 ± 0.07 [62], about 1.2σ lower than that measured in $B^0 \rightarrow J/\psi K^0$ decays. Belle II is expected to reduce this error by almost an order of magnitude, making the test much more sensitive.

The $B^0 \rightarrow K^0 \pi^0$ CP asymmetry is an important component of a sum rule which holds in the isospin limit [63]

$$\mathcal{A}_{K^+ \pi^-} \frac{\mathcal{B}_{K^+ \pi^-}}{\tau_{B^0}} + \mathcal{A}_{K^0 \pi^+} \frac{\mathcal{B}_{K^0 \pi^+}}{\tau_{B^+}} = 2\mathcal{A}_{K^+ \pi^0} \frac{\mathcal{B}_{K^+ \pi^0}}{\tau_{B^+}} + 2\mathcal{A}_{K^0 \pi^0} \frac{\mathcal{B}_{K^0 \pi^0}}{\tau_{B^0}}, \quad (1.5)$$

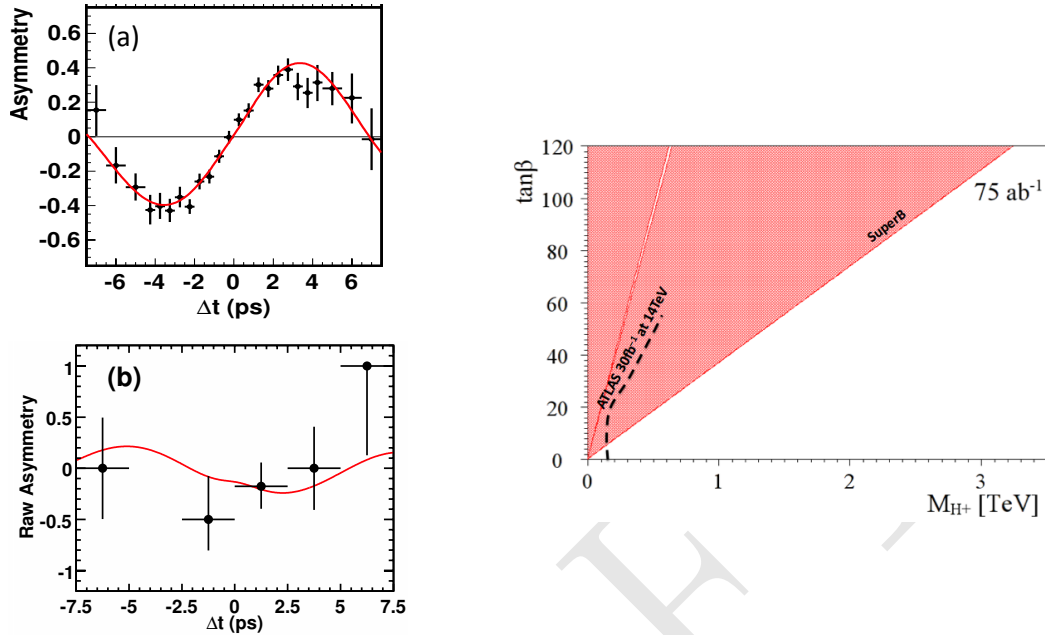


Figure 1-4. Left: Belle measurements of the time-dependent CP asymmetry versus Δt for (a) $B \rightarrow J/\psi K^0$ and (b) $B \rightarrow K_S^0 K_S^0$. The parameter $\sin(2\beta)$ is determined from the amplitude of the oscillations. Belle II should obtain statistics for $B \rightarrow K_S^0 K_S^0$ (and other loop-dominated modes) comparable to those obtained by Belle for $B \rightarrow J/\psi K^0$. Right: The expected constraint in m_H vs. $\tan\beta$ parameter space for a Type II Higgs doublet model that would result from 75 ab^{-1} of data at a super-B-factory. For comparison, also shown is the expected constraint from ATLAS in 30 fb^{-1} of data.

585 where \mathcal{A} denotes a CP asymmetry, \mathcal{B} a branching fraction, and τ a lifetime. This sum rule is thought to
 586 be accurate to a few percent precision and provides a robust test of the SM. The limitation of the test is
 587 the precision of $\mathcal{A}_{K^0\pi^0}$, which is difficult to measure and currently known to only $\sim 14\%$ precision [64]. At
 588 Belle II this is expected to be reduced to $\sim 3\%$ precision, greatly improving the sensitivity of Eq. (1.5) to NP.

589 Numerous rare B decays that were observed with low statistics by Belle and *BABAR* or not at all will become
 590 accessible at Belle II. One example is $B^+ \rightarrow \tau^+ \nu$, which in the SM results from a W -exchange diagram and
 591 has an expected branching fraction of $(0.76_{-0.06}^{+0.10}) \times 10^{-4}$ [65]. This mode is sensitive to supersymmetric
 592 models and others that predict the existence of a charged Higgs. The final state contains multiple neutrinos
 593 and thus is feasible to study only at an e^+e^- experiment. The current average branching fraction from Belle
 594 and *BABAR* is $(1.15 \pm 0.23) \times 10^{-4}$ [66, 67, 68, 69], somewhat higher than the SM expectation. Belle II should
 595 reduce this error to about 0.04×10^{-4} . The contribution of a charged Higgs boson within the context of a
 596 Type II Higgs doublet model (e.g., which is also the tree level Higgs sector of the Minimal Supersymmetric
 597 Model) would increase the branching fraction above the SM prediction by a factor $1 - (m_B^2/m_H^2) \tan^2 \beta$,
 598 where m_H is the mass of the charged Higgs and $\tan\beta$ is the ratio of vacuum expectation values of up-type
 599 and down-type Higgses. This relation can be used in conjunction with the measured value of the branching
 600 fraction to constrain m_H and $\tan\beta$. The expected constraint from a B -factory experiment with 75 ab^{-1} of
 601 data is shown in Fig. 1-4 (right). One sees that a large region of phase space is excluded. For $\tan\beta \gtrsim 60$,
 602 the range $m_H < 2 \text{ TeV}/c^2$ is excluded.

603 Other interesting processes include $b \rightarrow s\ell^+\ell^-$ and $b \rightarrow d\ell^+\ell^-$, with $\ell = e$ or μ . These are also sensitive to
 604 NP via loop diagrams. Belle II will reconstruct a broad range of exclusive final states such as $B \rightarrow K^{(*)}\ell^+\ell^-$,
 605 from which one can determine CP asymmetries, forward-backward asymmetries, and isospin asymmetries

606 (i.e., the asymmetry between $B^+ \rightarrow K^{(*)+}\ell^+\ell^-$ and $B^0 \rightarrow K^{(*)0}\ell^+\ell^-$). Belle II will also measure inclusive
 607 processes such as $B \rightarrow X_{s+d}\ell^+\ell^-$, for which theoretical predictions have less uncertainty than those for
 608 exclusive processes. By running on the $\Upsilon(5S)$ resonance, Belle II can study B_s^0 decays. Topical decay modes
 609 include $B_s^0 \rightarrow D_s^{*+}D_s^{*-}$, $D_s^{*+}\rho^-$, and $B_s^0 \rightarrow \gamma\gamma$, all of which are challenging in a hadronic environment.

610 The SuperKEKB project at KEK is well underway. Commissioning of the accelerator is expected to begin
 611 in 2015. The high luminosity ($8 \times 10^{35} \text{ cm}^{-2}\text{s}^{-1}$, 40 times larger than KEKB) results mainly from a smaller
 612 β^* function and reduced emittance. As a result, the vertical beam spread at the interaction point will shrink
 613 from $\sim 2 \mu\text{m}$ at KEKB to $\sim 60 \text{ nm}$ at SuperKEKB. In addition, the beam currents will be approximately
 614 doubled, and the beam-beam parameter will be increased by 50%.

615 The Belle II detector will be an upgraded version of the Belle detector that can handle the increased
 616 backgrounds associated with higher luminosity. The inner vertex detector will employ DEPLETED Field Effect
 617 (DEPFET) pixels located inside a new silicon strip tracker employing the APV25 ASIC (developed for
 618 CMS) to handle the large rates. There will also be a new small-cell drift chamber. The particle identification
 619 system will consist of an “imaging-time-of-propagation” (iTOP) detector in the barrel region, and an aerogel-
 620 radiator-based ring-imaging Cherenkov detector in the forward endcap region. The iTOP operates in a
 621 similar manner as BABAR’s DIRC detector, except that the photons are focused with a spherical mirror onto
 622 a finely segmented array of multi-channel-plate (MCP) PMTs. These MCP PMTs provide precise timing,
 623 which significantly improves the discrimination power between pions and kaons over that provided by imaging
 624 alone. The CsI(Tl) calorimeter will be retained but instrumented with waveform sampling readout. The
 625 innermost layers of the barrel K_L^0/μ detector, and all layers of the endcap K_L^0/μ detector, will be upgraded
 626 to use scintillator in order to accommodate the higher rates. Belle II should be ready to roll in by the spring
 627 of 2016 after commissioning of SuperKEKB is completed. The US groups on Belle II are focusing their
 628 efforts on the iTOP and K_L^0/μ systems.

629 1.4.3 Physics potential of hadronic experiments

630 LHCb and its upgrade

631 The spectacular successes of LHCb have realized some of the great potential for studying the decays of particles
 632 containing *c* and *b* quarks at hadron colliders. The production cross sections are quite large and the machine
 633 luminosities are very high, so more than 100 kHz of *b*-hadrons within the detector acceptance can be produced
 634 even at reduced LHC luminosities ($4 \times 10^{32} \text{ cm}^{-2}\text{s}^{-1}$). This is a much higher production rate than can be
 635 achieved even in the next generation e^+e^- *B* factories. All species of *b*-flavored hadrons, including B_s and B_c
 636 mesons, and *b* baryons, are produced. However, compared to e^+e^- colliders, the environment is much more
 637 harsh for experiments. At hadron colliders, the *b* quarks are accompanied by a very high rate of background
 638 events; they are produced over a very large range of momenta and angles; and even in *b*-events of interest
 639 there is a complicated underlying event. The overall energy of the center of mass of the hard scatter that
 640 produces the *b* quark, which is usually from the collision of a gluon from each beam particle, is not known,
 641 so the overall energy constraint that is so useful in e^+e^- colliders is not available. These features translate
 642 into challenges in triggering, flavor tagging, photon detection and limit the overall efficiency.

643 The CDF and D0 experiments at the Fermilab Tevatron demonstrated that these problems could be success-
 644 fully addressed using precision silicon vertex detectors and specialized triggers. While these experiments were
 645 mainly designed for high- p_T physics, they made major contributions to bottom and charm physics [70, 71].

646 The LHC produced its first collisions at 7 TeV center of mass energy at the end of March 2010. The b cross
647 section at the LHC is $\sim 300\mu\text{b}$, a factor of three higher than at the Tevatron and approximately 0.5% of the
648 inelastic cross section. When the LHC reaches its design center of mass energy of 14 TeV in 2015, the cross
649 section will be a factor of two higher.

650 The LHC program features for the first time at a hadron collider a dedicated B -physics experiment,
651 LHCb [72]. LHCb covers the forward direction from about 10 mr to 300 mr with respect to the beam
652 line. B hadrons in the forward direction are produced by collisions of gluons of unequal energy, so that
653 the center of mass of the collision is Lorentz boosted in the direction of the detector. Because of this, the
654 b -hadrons and their decay products are produced at small angles with respect to the beam and have momenta
655 ranging from a few GeV/ c to more than a hundred GeV/ c . Because of the Lorentz boost, even though the
656 angular range of LHCb is small, its coverage in pseudorapidity is between about 2 – 5, and both b hadrons
657 travel in the same direction, making b flavor tagging possible. With the small angular coverage, LHCb can
658 stretch out over a long distance along the beam without becoming too large transversely. A silicon microstrip
659 vertex detector (VELO) only 8 mm from the beam provides precision tracking that enables LHCb to separate
660 weakly decaying particles from particles produced at the interaction vertex. This allows the measurement of
661 lifetimes and oscillations due to flavor mixing. A 4 Tm dipole magnet downstream of the collision region, in
662 combination with the VELO, large area silicon strips (TT) placed downstream of the VELO but upstream of
663 the dipole, and a combination of silicon strips (IT) and straw tube chambers (OT) downstream of the dipole
664 provides a magnetic spectrometer with excellent mass resolution. There are two Ring Imaging Cherenkov
665 counters, one upstream of the dipole and one downstream, that together provide K - π separation from 2
666 to 100 GeV/ c . An electromagnetic calorimeter (ECAL) follows the tracking system and provides electron
667 triggering and π^0 and γ reconstruction. This is followed by a hadron calorimeter (HCAL) for triggering on
668 hadronic final states. A muon detector at the end of the system provides muon triggering and identification.

669 LHCb has a very sophisticated trigger system [73] that uses hardware at the lowest level (L0) to process the
670 signals from the ECAL, HCAL and muon systems. The L0 trigger reduces the rate to ~ 1 MHz followed by
671 the High Level Trigger (HLT), a large computer cluster, that reduces the rate to ~ 3 kHz for archiving to
672 tape for physics analysis. LHCb is able to run at a luminosity of $4.0 \times 10^{32} \text{ cm}^{-2} \text{ s}^{-1}$. This is much smaller
673 than the current peak luminosity achieved by the LHC and only a few percent of the LHC design luminosity.
674 The luminosity that LHCb can take efficiently is currently limited by the 1 MHz bandwidth between the
675 Level 0 trigger system and the trigger cluster. Therefore, the physics reach of LHCb is determined by the
676 detector capabilities and not by the machine luminosity. In fact, LHC implemented a “luminosity leveling”
677 scheme in the LHCb collision region so that LHCb could run at its desired luminosity throughout the store
678 while the other experiments, CMS and ATLAS, could run at higher luminosities. This mode of running will
679 continue until 2017 when a major upgrade [74, 75] of the LHCb trigger and parts of the detector and front end
680 electronics will increase the bandwidth to the HLT, increase archiving rate to 20 kHz, and permit operation
681 at a factor of 10 higher luminosity. Several subdetectors will be rebuilt for more robust performance at
682 higher luminosities, including VELO (pixels), TT (finer strips), IT+OT (technology to be soon decided) and
683 RICH (redesigned optics, MaPMTs).

684 There have been three runs of the LHC. In the first “pilot” run in 2010, LHCb recorded 35 pb^{-1} , which
685 was enough to allow it to surpass in precision many existing measurements of B decays. In 2011, the LHC
686 delivered more than 5 fb^{-1} to CMS and ATLAS. Since this luminosity was more than LHCb was designed to
687 handle, the experiment ran at a maximum luminosity that was 10% of the LHC peak luminosity. The total
688 integrated luminosity was about 1 fb^{-1} . In 2012 LHC delivered 20 fb^{-1} to CMS and ATLAS with additional
689 2 fb^{-1} collected by LHCb. Until the LHCb upgrade is installed in the long shutdown planned in 2018, LHCb
690 plans to run at a luminosity of $4.0 \times 10^{32} \text{ cm}^{-2} \text{ s}^{-1}$. Between now and then, LHCb will accumulate about
691 $1\text{--}2 \text{ fb}^{-1}$ per operating year, so a total of about 6.5 fb^{-1} will be obtained. The sensitivity will increase by
692 more than this because the LHC will run at 14 TeV, with about a factor of two higher B cross section. After

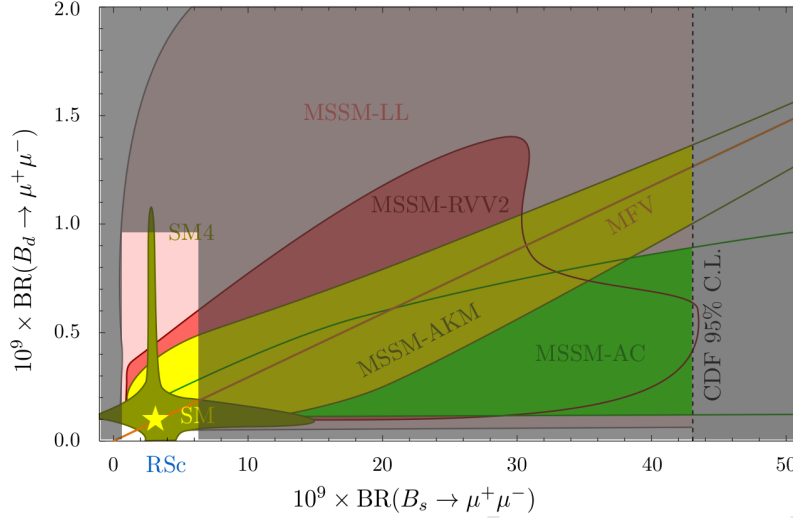


Figure 1-5. Correlation between the branching ratios of $B_s^0 \rightarrow \mu^+\mu^-$ and $B_d^0 \rightarrow \mu^+\mu^-$ in various models. The SM point is marked by a star. From Ref. [80] with the 2.1 fb^{-1} correction LHCb result [45] superimposed.

693 the upgrade is installed, LHCb will integrate about 5 fb^{-1} per year, so that about 50 fb^{-1} will be obtained
 694 over the decade following the upgrade installation.

695 The decay $B_s \rightarrow J/\psi\phi$ has been used to measure the CKM angle $\phi_s (\equiv -2\beta_s)$ [44]. The result, using also
 696 the decay mode $B_s \rightarrow J/\psi f_0$ [76] first established by LHCb [77], is $\phi_s = 0.01 \pm 0.07 \pm 0.01 \text{ rad}$ [44]. The
 697 difference in the width of the CP-even and CP-odd B_s mesons is $\Delta\Gamma_s = (0.106 \pm 0.011 \pm 0.007) \text{ ps}^{-1}$. These
 698 results are consistent with the SM, resolving a slight tension with earlier measurements from the Tevatron,
 699 which deviated somewhat from the SM predictions. However, the experimental uncertainty on ϕ_s is still a
 700 factor of 40 larger than that on the SM prediction, so improved measurements will probe higher mass scales
 701 of possible NP contributions.

702 The rare decay $B_s \rightarrow \mu^+\mu^-$ is predicted in the SM to have a branching fraction $(3.54 \pm 0.30) \times 10^{-9}$ [46, 47]. A
 703 higher or lower branching fraction would be an indicator for NP. LHCb presented first evidence of this decay
 704 based on 2.1 fb^{-1} of data, with $\mathcal{B}(B_s \rightarrow \mu^+\mu^-) = (3.2_{-1.2}^{+1.5}) \times 10^{-9}$ [45] consistent with the SM prediction.
 705 LHCb has recently updated its result for 3 fb^{-1} of data to $\mathcal{B}(B_s \rightarrow \mu^+\mu^-) = (2.9_{-1.0}^{+1.1}) \times 10^{-9}$ [49]. (CMS
 706 has also recently reported a measurement of $\mathcal{B}(B_s \rightarrow \mu^+\mu^-) = (3.0_{-0.9}^{+1.0}) \times 10^{-9}$ [48].) LHCb has also set
 707 an upper limit on $\mathcal{B}(B_d \rightarrow \mu^+\mu^-) < 0.74 \times 10^{-9}$ (95% C.L.) with the 3 fb^{-1} data set. These measurements
 708 impose stringent constraints on SUSY models as illustrated in Fig. 1-5. Further increase in statistics will
 709 probe even higher energy scales.

710 LHCb has also produced results on the key decay $B^0 \rightarrow K^{*0}\mu^+\mu^-$ (1.1 fb^{-1}) [81] that could reveal evidence
 711 for NP. One of the interesting observables is the forward-backward asymmetry of the μ^- relative to the
 712 direction of the parent B^0 meson in the dimuon center of mass vs. q^2 (dimuon invariant mass). The SM
 713 prediction crosses zero within a well-determined narrow region of q^2 , due to the interference between the SM
 714 box and electroweak penguin diagrams. NP can remove the crossover or displace its location. Indications
 715 from low statistics at Belle, BABAR, and CDF seemed to indicate that this might be happening. The LHCb
 716 results are the most precise so far, and are in good agreement with the SM within errors, which however can
 717 be significantly reduced with the LHCb upgrade. Many other observables sensitive to NP have also been
 718 investigated. The CMS (5.2 fb^{-1} [82]) and ATLAS (4.9 fb^{-1} [83]) Collaborations have also performed such
 719 studies. The results agree with the SM and the previous measurements, but have larger errors than LHCb.

Observable	SM theory uncertainty	Precision as of 2013	LHCb (6.5 fb ⁻¹)	LHCb Upgrade (50 fb ⁻¹)
$2\beta_s(B_s \rightarrow J/\psi\phi)$	~ 0.003	0.09	0.025	0.008
$\gamma(B \rightarrow D^{(*)}K^{(*)})$	$< 1^\circ$	8°	4°	0.9°
$\gamma(B_s \rightarrow D_s K)$	$< 1^\circ$	—	$\sim 11^\circ$	2°
$\beta(B^0 \rightarrow J/\psi K_S^0)$	small	0.8°	0.6°	0.2°
$2\beta_s^{\text{eff}}(B_s \rightarrow \phi\phi)$	0.02	1.6	0.17	0.03
$2\beta_s^{\text{eff}}(B_s \rightarrow K^{*0}\bar{K}^{*0})$	< 0.02	—	0.13	0.02
$2\beta_s^{\text{eff}}(B_s \rightarrow \phi\gamma)$	0.2%	—	0.09	0.02
$2\beta_s^{\text{eff}}(B^0 \rightarrow \phi K_S^0)$	0.02	0.17	0.30	0.05
A_{SL}^s	0.03×10^{-3}	6×10^{-3}	1×10^{-3}	0.25×10^{-3}
$\mathcal{B}(B_s \rightarrow \mu^+\mu^-)$	8%	42%	15%	5%
$\mathcal{B}(B^0 \rightarrow \mu^+\mu^-)/\mathcal{B}(B_s \rightarrow \mu^+\mu^-)$	5%	—	$\sim 100\%$	$\sim 35\%$
$A_{\text{FB}}(B^0 \rightarrow K^{*0}\mu^+\mu^-)$ zero crossing	7%	18%	6%	2%

Table 1-4. Sensitivity of LHCb to key observables. The current sensitivity (based on 1–3 fb⁻¹, depending on the measurement) is compared to that expected after 6.5 fb⁻¹ and that achievable with 50 fb⁻¹ by the upgraded experiment assuming $\sqrt{s} = 14$ TeV. Note that at the upgraded LHCb, the yield per fb⁻¹, especially in hadronic B and D decays, will be higher on account of the software trigger. (Adapted from Ref. [74].)

Many other decays are being studied, including all-hadronic decays such as $B_s \rightarrow \phi\phi$ [84] (β_s^{eff} via interference of mixing and decay via gluonic penguin) $B \rightarrow D\pi$, $B \rightarrow DK$ (determination of γ from tree processes), and states with photons such as $B_s \rightarrow \phi\gamma$ (search for right-handed currents). The expected sensitivity to selected important B decays during the present and upgraded phases of the LHCb experiment is shown in Table 1-4. In addition, LHCb has also demonstrated the capability for a rich program of studies of B_c meson decays.

The physics output of LHCb also extends beyond its B and charm (see next section) core programs. Examples of other topics include measurements of the production of electroweak gauge bosons in the forward kinematic region covered by the LHCb acceptance [85], studies of double parton scattering [86], measurements of the properties of exotic hadrons [87, 88], searches for lepton number and lepton flavor violations [89, 90] and for long-lived new particles [91].

ATLAS and CMS

Two LHC detectors, CMS and ATLAS, are designed to explore high mass and high- p_T phenomena to look for new physics at the LHC. They must operate at luminosities of up to 10^{34} cm⁻²s⁻¹, which implies the need to handle an average event pileup of ~ 20 . Both experiments can implement muon triggers with relatively low thresholds of a few GeV/ c . However, the rate of low- p_T muons from B decays competes for scarce resources with the many other trigger signatures that could contain direct evidence of new physics. Thus in practice, only B final states containing dimuons are well preserved through the trigger pipelines. The trigger efficiency is lower than in LHCb but at higher luminosity. One example of this, discussed above, is the rare decay $B_{d,s} \rightarrow \mu^+\mu^-$. CMS has very recently reported a measurement of $\mathcal{B}(B_s \rightarrow \mu^+\mu^-) = (3.0_{-0.9}^{+1.0}) \times 10^{-9}$ [48]. If ATLAS and CMS can maintain their trigger efficiency as the LHC luminosity and energy increase, they can be competitive in this study. The decay $B^0 \rightarrow K^{*0}\mu^+\mu^-$ presents more problems. The muons are softer and more difficult to trigger on and the limited K - π separation increases the background to the K^* . However,

742 as illustrated by their preliminary results these two experiments can play a confirming role to LHCb in this
 743 study. Despite their limitations, these two experiments will collect large numbers of B decays and should be
 744 able to observe many new decay modes and new particles containing b and charm quarks.

745 1.5 Report of the Charm Task Force

746 1.5.1 Introduction to Charm Physics

747 Studies of charm quarks can be split into two broad categories. First, in indirect searches for new physics
 748 affecting decays and oscillations, charm quarks furnish a unique probe of flavor physics in the up-quark
 749 sector, complementing strange and bottom physics. Second, as a probe of quantum chromodynamics (QCD)
 750 charm aids our understanding of nonperturbative physics, since it is not much heavier than the characteristic
 751 scale $\Lambda \sim 1$ GeV of QCD. Overall, charm adds much to the core new physics thrusts in heavy flavor physics
 752 while also adding significant breadth to the program.

753 Charm physics measurements allow for direct determination of the Cabibbo-Kobayashi-Maskawa (CKM)
 754 matrix elements $|V_{cs}|$ and $|V_{cd}|$, can also help improve the accuracy of $|V_{cb}|$ and $|V_{ub}|$ determined from B
 755 decays, and $|V_{ts}|$ and $|V_{td}|$ from B^0 and B_s^0 mixing. Part of this richness is due to the usefulness of charm
 756 data in verifying lattice QCD (LQCD) results.

757 Indirect searches for new physics with charm quarks provide competitive as well as complementary constraints
 758 to the results of direct searches at the Energy Frontier. One can classify searches in three broad categories,
 759 according to their “standard model background.”

760 1. Searches in the processes that are allowed in the standard model.

761 New physics contributions may often be difficult to discern in this case, except in cases of sufficient
 762 theoretical precision (e.g., leptonic decays of D mesons, $D_q \rightarrow \ell\bar{\nu}$). Alternatively, testing relations that
 763 are only valid in the standard model, but not in BSM models, may prove advantageous; e.g., CKM
 764 triangle relations.

765 2. Searches in the processes that are forbidden in the standard model at tree level.

766 Flavor-changing neutral current (FCNC) interactions occur in the standard model only through loops
 767 and are therefore suppressed. New physics contributions can enter both at tree-level and from one-
 768 loop corrections. Examples include $D^0 - \bar{D}^0$ mixing, or inclusive and exclusive transitions mediated
 769 by $c \rightarrow u\gamma$ or $c \rightarrow u\ell\bar{\ell}$.

770 Searches for CP violation in charm decays and oscillations should be included here as well, as they
 771 require at least two different pathways to reach the final state, at least one of which is FCNC transition.

772 3. Searches in the processes that are forbidden in the standard model.

773 While these processes are generally very rare even in NP models, their observation, however, would
 774 constitute a high-impact discovery. Examples include searches for lepton- and baryon-number-violating
 775 transitions, such as $D^0 \rightarrow e^+\mu^-$, $D^0 \rightarrow \bar{p}e^+$, etc.

776 The QCD side of charm physics is also very vibrant. Recently, there has been much activity in “XYZ” state
 777 spectroscopy, in addition to continued studies of conventional charmonium. This provides a rich source of
 778 results in hadronic physics and radiative transitions.

1.5.2 Current and Future Experiments

Over the past decade, charm results have been dominated by results from detectors at the e^+e^- “flavor factories” BaBar, Belle, and CLEO-c. Currently, the BESIII experiment is running at charm threshold and Belle II, which will run at and near the $\Upsilon(4S)$, is under construction; both experiments have excellent capabilities in charm [92, 55]. While charm statistics are lower at threshold, the data are unique in their ability to measure strong phases and also excel at modes with neutrinos in the final state. The Belle II detector should begin physics running in 2016; charm from continuum fragmentation at B -factory energies is complementary to threshold data.

At hadron machines, CDF was able to contribute due to displaced-vertex and muon triggers, producing notable results on $D^0 - \bar{D}^0$ oscillations. While muon triggers have produced some charm results from ATLAS and CMS, the current and future charm program at hadron colliders lies almost exclusively with the dedicated flavor experiment, LHCb. Many areas of charm physics are accessible at LHCb and the 2018 upgrade will enhance opportunities even more. Their physics reach [74, 93] is an important addition to the e^+e^- program.

The BESIII program should continue at least until the end of the decade, and Belle II and LHCb will carry charm physics well into the 2020’s. One major decision point is the future of threshold charm after BESIII. Currently, the Cabibbo Lab near Rome is preparing a threshold tau-charm factory proposal. Interest has also been expressed by BINP at Novosibirsk and institutions in Turkey.

Leptonic and Semileptonic Decays and CKM triangle relations

In leptonic and semileptonic decays, all of the uncertainties from strong-interaction effects may be conveniently parametrized as decay constants and form factors, respectively. The remainder of the theory is straightforward weak-interaction physics. Indeed, comparing decay constants and form factors to LQCD predictions allows one to exclude large portions of parameter space for NP models with charged scalars.

Leptonic decay rates depend on the square of both decays constants and CKM matrix elements. If one uses LQCD as in input, then $|V_{cq}|$ may be extracted. If the CKM matrix elements are taken from elsewhere (possibly unitarity constraints), then we can test LQCD results. In fact, by taking ratios of leptonic and semileptonic decays, one can cancel $|V_{cq}|$ to obtain pure LQCD tests.

The Cabibbo-suppressed leptonic decay $D^+ \rightarrow \mu\nu$ is only measurable at threshold charm machines. Currently, it is essentially determined via one CLEO-c result [94], although BESIII has a preliminary result based on a dataset 3.5 times larger [95]. This result, $f_D = (203.91 \pm 5.72 \pm 1.91)$ MeV, based on 2.9 fb^{-1} , is still statistics-limited.

The Cabibbo-favored $D_s^+ \rightarrow \mu\nu, \tau\nu$ process is easier in two respects. Unlike the D^+ case, where $\tau\nu$ is a relatively small effect, here it offers additional channels that enhance the utility of a dataset. In addition, B factories possess enough tagging power in continuum charm production to make the best current single measurement. The one drawback is that D_s production rates are smaller than D^+ . Currently, the best measurement of f_{D_s} is a preliminary result from Belle [96].

Successful LQCD calculations of $D_{(s)}$ decay constants will give confidence in their results for B decay constants. And while f_B can be obtained from $B \rightarrow \tau\nu$, there is no analogous direct way to determine f_{B_s} . By contrast, in charm, both strange and non-strange decay constants are directly accessible.

818 The key semileptonic modes are $D^0 \rightarrow K^- e^+ \nu$, $\pi^- e^+ \nu$. Additional statistical power may be obtained by
 819 including the isospin-related D^+ decays, but both CKM matrix elements are accessible without the need
 820 for the more experimentally challenging D_s decays. The form factors, $f_K(q^2)$ and $f_\pi(q^2)$, are useful tests of
 821 LQCD. One depends on similar LQCD calculations to extract $|V_{ub}|$ from $B \rightarrow \pi \ell \nu$ decays.

822 For leptonic charm decays, $f_{D(s)}$ parametrizes the probability that the heavy and light quarks “find each
 823 other” to annihilate. Due to helicity suppression the rate goes as m_ℓ^2 , and many NP models could have a
 824 different parametric dependence on m_ℓ^2 . New physics can be discussed in terms of generalized couplings [97].
 825 Models probed by this decay include extended Higgs sectors, which contain new charged scalar states, or
 826 models with broken left-right symmetry, which include heavy vector W_R^\pm states.

827 One can also search for new physics by testing relations that hold in the SM, but not necessarily in general.
 828 An example of such relation is a CKM “charm unitarity triangle” relation:

$$V_{ud}^* V_{cd} + V_{us}^* V_{cs} + V_{ub}^* V_{cb} = 0. \quad (1.6)$$

829 Processes that are used to extract CKM parameters in Eq. (1.6) can be affected by new physics. This can
 830 lead to disagreement between CKM elements extracted from different processes, or the triangle not closing.
 831 Finally, since all CP-violating effects in the flavor sector of the SM are related to the single phase of the
 832 CKM matrix, all of the CKM unitarity triangles, have the same area, $A = J/2$, where J is the Jarlskog
 833 invariant. This fact could provide a non-trivial check of the standard model, given measurements of more
 834 than one triangle with sufficient accuracy. Unfortunately, the “charm triangle” will be harder to work with
 835 than the familiar B physics triangle since it is rather “squashed.” In terms of the Wolfenstein parameter
 836 $\lambda = 0.22$, the relation in Eq. (1.6) has one side $\mathcal{O}(\lambda^5)$ with the other two being $\mathcal{O}(\lambda)$.

837 D^0 Oscillations (including CP Violation)

838 The presence of $\Delta C = 2$ operators produce off-diagonal terms in the $D^0 - \bar{D}^0$ mass matrix, mixing the flavor
 839 eigenstates into the mass eigenstates

$$|D_{1,2}\rangle = p|D^0\rangle \pm q|\bar{D}^0\rangle. \quad (1.7)$$

840 Neglecting CP violation leads to $|p| = |q| = 1/\sqrt{2}$. The mass and width splittings between the mass
 841 eigenstates are

$$x = \frac{m_1 - m_2}{\Gamma_D}, \quad y = \frac{\Gamma_1 - \Gamma_2}{2\Gamma_D}, \quad (1.8)$$

842 where Γ_D is the average width of the two mass eigenstates.

843 The oscillation parameters x and y are both of order 1% in the D^0 system. These small values require the
 844 high statistics of B factories and hadron machines. Observations thus far have relied on the time-dependence
 845 of several hadronic decays $K\pi$, $K\pi\pi^-$, $K_S\pi\pi$, etc., as well as lifetime differences between CP-eigenstate
 846 decays (KK , $\pi\pi$) and the average lifetime (see the review in [61]). LHCb has made the highest significance
 847 (9σ) observation of D^0 oscillations in a single experiment [98]. However, a non-zero value of x has not yet
 848 been established at 3σ . LHCb and Belle II will be able to pinpoint the value of x in the next several years.

849 Theoretical predictions for x and y in the SM are uncertain, although values as high as 1% had been
 850 expected [99]. The predictions need to be improved, and several groups are working to understand the
 851 problem using technology such as the heavy-quark expansion, lattice QCD, and other long-distance methods.

852 However, one can place an upper bound on the NP parameters by neglecting the SM contribution altogether
 853 and assuming that NP saturates the experimental result. One subtlety is that the SM and NP contributions
 854 can have either the same or opposite signs. While the sign of the SM contribution cannot be calculated

reliably due to hadronic uncertainties, x computed within a given NP model can be determined. This stems from the fact that NP contributions are generated by heavy degrees of freedom, making the short-distance calculation reliable.

Any NP degree of freedom will generally be associated with a generic heavy mass scale M , at which the NP interaction is most naturally described. At the scale m_c , this description must be modified by the effects of QCD. In order to see how NP might affect the mixing amplitude, it is instructive to consider off-diagonal terms in the neutral D mass matrix,

$$M_{12} - \frac{i}{2} \Gamma_{12} = \frac{1}{2M_D} \langle \bar{D}^0 | \mathcal{H}_w^{\Delta C=-2} | D^0 \rangle + \frac{1}{2M_D} \sum_n \frac{\langle \bar{D}^0 | \mathcal{H}_w^{\Delta C=-1} | n \rangle \langle n | \mathcal{H}_w^{\Delta C=-1} | D^0 \rangle}{M_D - E_n + i\epsilon}, \quad (1.9)$$

where the first term contains $\mathcal{H}_w^{\Delta C=-2}$, which is an effective $|\Delta C| = 2$ Hamiltonian, represented by a set of operators that are local at the $\mu \sim m_D$ scale. This first term only affects x , but not y .

As mentioned above, heavy BSM degrees of freedom cannot be produced in charm meson decays, but can nevertheless affect the effective $|\Delta C| = 2$ Hamiltonian by changing Wilson coefficients and introducing new operator structures. By integrating out those new degrees of freedom associated with a high scale M , we are left with an effective Hamiltonian written in the form of a series of operators of increasing dimension. It turns out that a model-independent study of NP $|\Delta C| = 2$ contributions is possible, as any NP model will only modify Wilson coefficients of those operators [100, 101],

$$\mathcal{H}_{\text{NP}}^{|\Delta C|=2} = \frac{1}{M^2} \sum_{i=1}^8 C_i(\mu) Q_i(\mu),$$

$$\begin{aligned} Q_1 &= (\bar{u}_L^\alpha \gamma_\mu c_L^\alpha) (\bar{u}_L^\beta \gamma^\mu c_L^\beta), & Q_5 &= (\bar{u}_R^\alpha c_L^\beta) (\bar{u}_L^\beta c_R^\alpha), \\ Q_2 &= (\bar{u}_R^\alpha c_L^\alpha) (\bar{u}_R^\beta c_L^\beta), & Q_6 &= (\bar{u}_R^\alpha \gamma_\mu c_R^\alpha) (\bar{u}_R^\beta \gamma^\mu c_R^\beta), \\ Q_3 &= (\bar{u}_R^\alpha c_L^\beta) (\bar{u}_R^\beta c_L^\alpha), & Q_7 &= (\bar{u}_L^\alpha c_R^\alpha) (\bar{u}_L^\beta c_R^\beta), \\ Q_4 &= (\bar{u}_R^\alpha c_L^\alpha) (\bar{u}_L^\beta c_R^\beta), & Q_8 &= (\bar{u}_L^\alpha c_R^\beta) (\bar{u}_L^\beta c_R^\alpha), \end{aligned} \quad (1.10)$$

where C_i are dimensionless Wilson coefficients, and the Q_i are the effective operators; α and β are color indices. In total, there are eight possible operator structures contributing to $|\Delta C| = 2$ transitions. Taking operator mixing into account, a set of constraints on the Wilson coefficients of Eq. (1.10) can be placed,

$$(|C_1|, |C_2|, |C_3|, |C_4|, |C_5|) \leq (57, 16, 58, 5.6, 16) \times 10^{-8} \left(\frac{M}{1 \text{ TeV}} \right)^2. \quad (1.11)$$

The constraints on $C_6 - C_8$ are identical to those on $C_1 - C_3$ [101]. Note that Eq. (1.11) implies that new physics particles have highly suppressed couplings to charm quarks. Alternatively, the tight constraints of Eq. (1.11) probe NP at the very high scales: $M \geq (4 - 10) \times 10^3$ TeV for tree-level NP-mediated charm mixing and $M \geq (1 - 3) \times 10^2$ TeV for loop-dominated mixing via new physics particles.

There is a beautiful effect at threshold, where the decay of the $\psi(3770)$ gives a quantum correlated $D^0 - \bar{D}^0$ pair, and like-sign $K^\pm \pi^\mp$ decays at equal times only arise from mixing, without the doubly-Cabibbo-suppressed background. However, this requires high-quality particle ID, and is very luminosity-intensive. The event rate is of order one event per 5 fb^{-1} (the current BESIII dataset is 2.9 fb^{-1}). Threshold does come into play in a different manner, however. When mixing is measured via the time dependence of hadronic decays, one measures x, y in a rotated basis. These parameters, denoted x', y' in the case of $K^\pm \pi^\mp$, can only be converted to the desired x, y with knowledge of a strong final-state scattering phase, $\delta_{K\pi}$. Threshold charm data provide the only possibility to measure this (and other related) phases.

CP violation in $D^0 - \bar{D}^0$ mixing is an important area for future work. In Table 1-5, we summarize the prospects for future results on these topics. The entries related to q/p parametrize CP violation; in the absence of CP violation in mixing, $|q/p| = 1$ and $\arg(q/p) = 0$ in the phase convention adopted.

Observable	Current Expt.	LHCb (5 fb ⁻¹)	Belle II (50 ab ⁻¹)	LHCb Upgrade (50 fb ⁻¹)
x	$(0.63 \pm 0.20)\%$	$\pm 0.06\%$	$\pm 0.02\%$	$\pm 0.02\%$
y	$(0.75 \pm 0.12)\%$	$\pm 0.03\%$	$\pm 0.01\%$	$\pm 0.01\%$
y_{CP}	$(1.11 \pm 0.22)\%$	$\pm 0.02\%$	$\pm 0.03\%$	$\pm 0.01\%$
$ q/p $	0.91 ± 0.17	± 0.085	± 0.03	± 0.03
$\arg(q/p)$	$(-10.2 \pm 9.2)^\circ$	$\pm 4.4^\circ$	$\pm 1.4^\circ$	$\pm 2.0^\circ$

Table 1-5. Sensitivities of Belle II and LHCb to charm mixing related parameters, along with the current results for these measurements; here $\arg(q/p)$ means $\arg[(q/p)(\bar{A}_{K^+K^-}/A_{K^+K^-})]$. The second column gives the 2011 world averages. The remaining columns give the expected accuracy at the indicated integrated luminosities. In the convention used in HFAG fits, in the absence of CP violation $|q/p| = 1$ and $\arg(q/p) = 0$.

888 CP Violation in Decays

889 A possible manifestation of new physics interactions in the charm system is associated with the observation
 890 of CP violation [102, 103]. This is due to the fact that all quarks that build up the hadronic states in weak
 891 decays of charm mesons belong to the first two generations. Since the 2×2 Cabibbo quark mixing matrix
 892 is real, no CP violation is possible in the dominant tree-level diagrams which describe the decay amplitudes.
 893 CP-violating amplitudes can be introduced in the standard model by including penguin or box operators
 894 induced by virtual b quarks. However, their contributions are strongly suppressed by the small combination
 895 of CKM matrix elements $V_{cb}V_{ub}^*$. Thus, it was believed that the observation of large CP violation in charm
 896 decays or mixing would be an unambiguous sign for new physics. The SM “background” here is quite small,
 897 giving CP-violating asymmetries of the order of 10^{-3} . Hence, observation of CP-violating asymmetries larger
 898 than 1% could indicate presence of new physics.

899 Recent measurements have indicated the possibility of direct CP violation in the decays $D^0 \rightarrow K^+K^-$ and
 900 $D^0 \rightarrow \pi^+\pi^-$ [104]. The current world average is

$$\Delta A_{CP} = A_{CP}(K^-K^+) - A_{CP}(\pi^-\pi^+) = -(0.33 \pm 0.12)\%, \quad (1.12)$$

901 although the most recent LHCb result (included in this average) has a central value with the opposite sign.
 902 These result triggered intense theoretical discussions of the possible size of this quantity in the standard
 903 model and in models of new physics [105]. New measurements of individual direct CP-violating asymmetries
 904 entering Eq. (1.12) and other asymmetries in the decays of neutral and charged D 's into PP , PV , and VV
 905 final states are needed to guide theoretical calculations (of penguin amplitudes).

906 It is also important to measure CP-violating asymmetries in the decays of charmed baryon states, as those
 907 could have different theoretical and experimental systematics and could provide a better handle on theoretical
 908 uncertainties.

909 No indirect CP violation has been observed in charm transitions yet. However, available experimental
 910 constraints can provide some tests of CP-violating NP models. For example, a set of constraints on the
 911 imaginary parts of Wilson coefficients of Eq. (1.10) can be placed,

$$(|\text{Im}C_1|, |\text{Im}C_2|, |\text{Im}C_3|, |\text{Im}C_4|, |\text{Im}C_5|) < (11, 2.9, 11, 1.1, 3.0) \times 10^{-8} \left(\frac{M}{1 \text{ TeV}}\right)^2. \quad (1.13)$$

912 Just like the constraints of Eq. (1.11), they give a sense of how NP particles couple to the standard model.

913 Rare Decays

914 The flavor-changing neutral current (FCNC) decay $D^0 \rightarrow \mu^+\mu^-$ is of renewed interest after the measurement
 915 of $B_s \rightarrow \mu^+\mu^-$. While heavily GIM-suppressed, long-distance contributions from $D^0 \rightarrow \gamma\gamma$, for example,
 916 also contribute. Direct knowledge of the decay $D^0 \rightarrow \gamma\gamma$ allows one to limit these contributions to the
 917 di-muon mode to below 6×10^{-11} .

918 Decays $B \rightarrow K^{(*)}\ell^+\ell^-$ have been the subject of great interest for many years, both rates and angular
 919 distributions offer the chance to see new physics effects. The analogous charm decays, $D_{(s)}^+ \rightarrow h^+\mu^+\mu^-$,
 920 $D^0 \rightarrow hh'\mu^+\mu^-$ are likewise interesting. The former modes have long-distance contributions of order 10^{-6}
 921 from vector intermediaries (ρ, ω, ϕ) but these can be cut away. The standard model rate for the remaining
 922 decays is around 10^{-11} . For the latter modes, one can form forward-backward and T -odd asymmetries with
 923 sensitivity to new physics.

924 Experimentally, at present, there are only the upper limits on $D^0 \rightarrow \ell^+\ell^-$ decays,

$$\mathcal{B}(D^0 \rightarrow \mu^+\mu^-) \leq 1.1 \times 10^{-8}, \quad \mathcal{B}(D^0 \rightarrow e^+e^-) \leq 7.9 \times 10^{-8}, \quad \mathcal{B}(D^0 \rightarrow \mu^\pm e^\mp) \leq 2.6 \times 10^{-7}. \quad (1.14)$$

925 Theoretically, just like in the case of mixing discussed above, all possible NP contributions to $c \rightarrow u\ell^+\ell^-$
 926 can also be summarized in an effective Hamiltonian,

$$\mathcal{H}_{\text{NP}}^{\text{rare}} = \sum_{i=1}^{10} \tilde{C}_i(\mu) \tilde{Q}_i, \quad \begin{aligned} \tilde{Q}_1 &= (\bar{\ell}_L \gamma_\mu \ell_L) (\bar{u}_L \gamma^\mu c_L), & \tilde{Q}_4 &= (\bar{\ell}_R \ell_L) (\bar{u}_R c_L), \\ \tilde{Q}_2 &= (\bar{\ell}_L \gamma_\mu \ell_L) (\bar{u}_R \gamma^\mu c_R), & \tilde{Q}_5 &= (\bar{\ell}_R \sigma_{\mu\nu} \ell_L) (\bar{u}_R \sigma^{\mu\nu} c_L), \\ \tilde{Q}_3 &= (\bar{\ell}_L \ell_R) (\bar{u}_R c_L), \end{aligned} \quad (1.15)$$

927 where \tilde{C}_i are again Wilson coefficients, and the \tilde{Q}_i are the effective operators. In this case, however, there
 928 are ten of them, with five additional operators $\tilde{Q}_6, \dots, \tilde{Q}_{10}$ that can be obtained from operators in Eq. (1.15)
 929 by the substitutions $L \rightarrow R$ and $R \rightarrow L$. Further details may be found in Ref. [106], where it is also noted
 930 that it might be advantageous to study correlations of new physics contributions to various processes, for
 931 instance $D^0 - \bar{D}^0$ mixing and rare decays.

932 Strong Phases

933 Threshold data with correlated $D^0 - \bar{D}^0$ pairs may be used to extract strong phases in D decays. These
 934 phases enter into B physics determinations of the CKM angle γ from $B \rightarrow D^{(*)}K^{(*)}$ decays [107]. Without
 935 direct input from charm, these B results suffer from ill-defined systematic uncertainties and lose precision.
 936 In addition, strong phases are needed to relate observables of $D^0 - \bar{D}^0$ oscillations measured with hadronic
 937 final states to the usual x, y parameters.

938 Charmonium and Spectroscopy

939 Recent observations of conventional charmonium states [108] such as the h_c and $\eta_c(2S)$ are accompanied by
 940 continuing discoveries of more “XYZ” exotic states [109].

941 The spectroscopy of conventional states can be used to calibrate LQCD, and many γ (both E1 and M1),
 942 $\pi^0, \eta, \pi\pi$ transitions have been studied. The XYZ states are a challenge to QCD, and may include tetra-
 943 quarks, $c\bar{c}g$ hybrids, meson molecules, etc. Experimental data continue to accumulate, giving more input to
 944 a vibrant field, testing many theoretical ideas.

945 Other Topics

946 We finally list a few topics on “engineering numbers.” Currently, charm lifetimes are dominated by FOCUS
947 results; while the results are well-respected, a cross-check would be welcome. These results serve to relate
948 theoretical predictions for partial widths to the experimentally accessible quantities, branching fractions.

949 Likewise, golden mode branching fractions for D mesons are dominated by CLEO-c; a cross-check from
950 BESIII is in order. For the baryons, where there are four weakly-decaying ground states, there are no
951 absolute branching fraction results. For $\Lambda_c \rightarrow pK^- \pi^+$, the near-threshold enhancement of Λ_c pairs measured
952 by Belle in ISR [110] shows that BESIII should be able to provide a nice result with a modest-length run.

953 In addition to topics discussed above, charm quarks will play a major role in the heavy-ion experimental
954 programs at RHIC and LHC for the next decade. Questions that will be addressed include identification of
955 the exact energy loss and hadronization mechanisms of charm (or beauty) quarks in propagation through
956 Quark-Gluon Plasma (QGP), calculations of heavy quark transport coefficients, etc.

957 1.5.3 Charm Physics Summary and Perspectives Beyond 2020

958 Continued support of BESIII, LHCb, and Belle II is critical to U.S. involvement in a vibrant charm program.
959 Investments in the first two are rather modest, yet provide valuable access to exciting datasets. Attention
960 should also be paid to possible opportunities at a future threshold experiment should one be built abroad.

961 Theoretical calculations in charm physics are mainly driven by experimental results. The challenges as-
962 sociated with nonperturbative QCD dynamics are being addressed by advances in lattice QCD and other
963 nonperturbative approaches. While similar probes of the NP scale that might reveal the “grand design”
964 of flavor are available in the strange and beauty systems, charm quarks furnish unique access to processes
965 involving up quarks, more precise and complementary to searches for FCNC top decays. Moreover, D mesons
966 are the only neutral mesons composed of up-type quarks which have flavor oscillations, and thus probe NP
967 in the $\Delta F = 2$ transitions, providing complementary sensitivity to K , B , and B_s mixing.

968 1.6 Report of the Lattice QCD Task Force

969 The properties of the five least massive quarks offer a powerful tool to indirectly study physics at energies
970 many orders of magnitude above those which are accessible to present or planned accelerators. This is
971 made possible in large part by the quarks’ strong interactions which provide experimental physics with a
972 host of bound states, common and rare decay processes and mixings that enable clever and highly sensitive
973 studies of the properties of the underlying quarks. Until recently, the lack of predictive control of these same
974 strong interactions provided a large barrier to fully exploiting this potential. Ab initio lattice calculations
975 are systematically removing this barrier, allowing us to fully exploit the strong interactions of the quarks to
976 search for physics beyond the standard model. In this section we describe the status and prospects for the
977 lattice QCD calculations needed for future quark-flavor experiments. Much of this material is drawn from a
978 recent USQCD (the national US lattice-QCD collaboration) white paper [111].

979 Lattice QCD provides a first-principles method for calculating low-energy hadronic matrix elements with
980 reliable and systematically-improvable uncertainties. Such matrix elements — decay constants, form factors,
981 mixing matrix elements, etc. — are needed to determine the standard model (SM) predictions for many
982 processes and/or to extract CKM matrix elements.

Quantity	CKM element	Present expt. error	2007 forecast lattice error	Present lattice error	2018 lattice error
f_K/f_π	$ V_{us} $	0.2%	0.5%	0.4%	0.15%
$f_+^{K\pi}(0)$	$ V_{us} $	0.2%	–	0.4%	0.2%
f_D	$ V_{cd} $	4.3%	5%	2%	< 1%
f_{D_s}	$ V_{cs} $	2.1%	5%	2%	< 1%
$D \rightarrow \pi \ell \nu$	$ V_{cd} $	2.6%	–	4.4%	2%
$D \rightarrow K \ell \nu$	$ V_{cs} $	1.1%	–	2.5%	1%
$B \rightarrow D^* \ell \nu$	$ V_{cb} $	1.3%	–	1.8%	< 1%
$B \rightarrow \pi \ell \nu$	$ V_{ub} $	4.1%	–	8.7%	2%
f_B	$ V_{ub} $	9%	–	2.5%	< 1%
ξ	$ V_{ts}/V_{td} $	0.4%	2–4%	4%	< 1%
Δm_s	$ V_{ts}V_{tb} ^2$	0.24%	7–12%	11%	5%
B_K	$\text{Im}(V_{td}^2)$	0.5%	3.5–6%	1.3%	< 1%

Table 1-6. History, status and future of selected lattice-QCD calculations needed for the determination of CKM matrix elements. 2007 forecasts are from Ref. [112]. Most present lattice results are taken from latticeaverages.org [113]. The quantity ξ is $f_{B_s} \sqrt{B_{B_s}} / (f_B \sqrt{B_B})$.

983 In the last five years lattice QCD has matured into a precision tool. Results with fully controlled errors are
 984 available for nearly 20 matrix elements: the decay constants f_π , f_K , f_D , f_{D_s} , f_B and f_{B_s} , semileptonic form
 985 factors for $K \rightarrow \pi$, $D \rightarrow K$, $D \rightarrow \pi$, $B \rightarrow D$, $B \rightarrow D^*$, $B_s \rightarrow D_s$ and $B \rightarrow \pi$, and the four-fermion mixing
 986 matrix elements B_K , $f_B^2 B_B$ and $f_{B_s}^2 B_{B_s}$. By contrast, in 2007 (when the previous USQCD white paper was
 987 written [112]), only f_K/f_π was fully controlled. A sample of present errors is collected in Table 1-6. For K
 988 mesons, errors are at or below the percent level, while for D and B mesons errors range from few to $\sim 10\%$.

989 The lattice community is embarking on a three-pronged program of future calculations: (i) steady but
 990 significant improvements in “standard” matrix elements of the type just described, leading to much improved
 991 results for CKM parameters (e.g., V_{cb}); (ii) results for many additional matrix elements relevant for searches
 992 for new physics and (iii) the extension of lattice methods to more challenging matrix elements which can
 993 both make use of old results and provide important information for upcoming experiments.

994 Reducing errors in the standard matrix elements has been a major focus of the lattice community over the last
 995 five years, and the improved results illustrated in Table 1-6 now play an important role in the determination
 996 of the CKM parameters in the “unitarity triangle fit.” Lattice-QCD calculations involve various sources
 997 of systematic error (the need for extrapolations to zero lattice spacing, infinite volume and the physical
 998 light-quark masses, as well as fitting and operator normalization) and thus it is important to cross-check
 999 results using multiple discretizations of the continuum QCD action. (It is also important to check that
 1000 results for the hadron spectrum agree with experiment. Examples of these checks are shown in the 2013
 1001 whitepaper [111].) This has been done for almost all the quantities noted above. This situation has spawned
 1002 two lattice averaging efforts, latticeaverages.org [113] and FLAG-1 [114], which have recently joined
 1003 forces and expanded to form a worldwide Flavor Lattice Averaging Group (FLAG-2), with first publication
 1004 expected in mid-2013.

1005 The ultimate aim of lattice-QCD calculations is to reduce errors in hadronic quantities to the level at which
 1006 they become subdominant either to experimental errors or other sources of error. As can be seen from

1007 Table 1-6, several kaon matrix elements are approaching this level, while lattice errors remain dominant
 1008 in most quantities involving heavy quarks. Thus the most straightforward contribution of lattice QCD to
 1009 the future intensity frontier program will be the reduction in errors for such quantities. Forecasts for the
 1010 expected reductions by 2018 are shown in the table. These are based on a Moore’s law increase in computing
 1011 power, and extrapolations using existing algorithms. Past forecasts have been typically conservative (as
 1012 shown in the table) due to unanticipated algorithmic or other improvements. The major reasons for the
 1013 expected reduction in errors are the use of u and d quarks with physical masses, the use of smaller lattice
 1014 spacings and improved heavy-quark actions, and the reduction in statistical errors.

1015 Thus one key contribution of lattice QCD to the future flavor-physics program will be a significant reduction
 1016 in the errors in CKM elements, most notably V_{cb} . This feeds into the SM predictions for several of the
 1017 rare decays that are part of the proposed experimental program, e.g., $K \rightarrow \pi\nu\bar{\nu}$. For these decays, the
 1018 parametric error from $|V_{cb}|$, which enters as the fourth power, is the dominant source of uncertainty in the SM
 1019 predictions. The lattice-QCD improvements projected in Table 1-6 will bring the theoretical uncertainties
 1020 to a level commensurate with the projected experimental errors in time for the planned rare kaon-decay
 1021 experiments at Fermilab.

1022 The matrix elements discussed so far involve only a single hadron and no quark-disconnected contractions.
 1023 These are the most straightforward to calculate (and are sometimes called “gold-plated”). The second part
 1024 of the future lattice-QCD program for the intensity frontier will be the extension of the calculations to
 1025 other, similar, matrix elements which are needed for the search for new physics. This includes the mixing
 1026 matrix elements for kaons, D and B mesons arising from operators present in BSM theories but absent in
 1027 the SM, the form factors arising in $B \rightarrow K\ell^+\ell^-$ and $\Lambda_b \rightarrow \Lambda\ell^+\ell^-$, non-SM form factors for $K \rightarrow \pi$, $B \rightarrow \pi$
 1028 and $B \rightarrow K$ transitions. We expect the precision attained for these quantities to be similar to those for
 1029 comparable quantities listed in Table 1-6.

1030 The third part of the lattice-QCD program is the least developed and most exciting. This involves the
 1031 development of new methods or the deployment of known but challenging methods, and allows a substantial
 1032 increase in the repertoire of lattice calculations. In particular, calculations involving two particles below
 1033 the inelastic threshold are now possible (e.g., $K \rightarrow \pi\pi$ amplitudes [115, 116, 117]), quark-disconnected
 1034 contractions are being controlled (e.g., η' and η masses [118] and the nucleon sigma term [119]) and
 1035 processes involving two insertions of electroweak operators are under pilot study (e.g., the long-distance
 1036 part of Δm_K [120]). During the next five years, we expect that these advances will lead to a quantitative
 1037 understanding of the $\Delta I = 1/2$ rule, a prediction with $\sim 5\%$ errors for the the SM contribution to ϵ'_K , and
 1038 predictions with 10–20% errors for the long-distance contributions to Δm_K and ϵ_K . This will finally allow
 1039 us to use these hallowed experimental results in order to search for new physics.

1040 These new methods should allow lattice QCD to contribute directly to the proposed flavor-physics ex-
 1041 periments. For example, a calculation of the long-distance contributions to $K \rightarrow \pi\nu\bar{\nu}$ decays should be
 1042 possible, checking the present estimate that these contributions are small. Similar methods should allow the
 1043 calculation of the sign of the CP-conserving amplitude $K_S \rightarrow \pi^0 e^- e^+$, thus resolving a major ambiguity in
 1044 the SM prediction for $K_L \rightarrow \pi^0 e^- e^+$.

1045 We also expect progress on even more challenging calculations, for which no method is yet known. An
 1046 important example, in light of recent evidence for CP violation in D decays and for $D - \bar{D}$ mixing, is to
 1047 develop a method for calculating the amplitudes for $D \rightarrow \pi\pi$, KK decays and $D - \bar{D}$ mixing. This requires
 1048 dealing with four or more particles in a finite box, as well as other technical details.

1049 These plans rely crucially on access to high-performance computing, as well as support for algorithm and
 1050 software development. In the US, much of this infrastructure is coordinated by the USQCD umbrella
 1051 collaboration. Continued support for this effort is essential for the program discussed here.

1052 We also stress that there are substantial lattice-QCD efforts underway to calculate the hadronic (vacuum
 1053 polarization and light-by-light) contributions to muonic $g - 2$, the light- and strange-quark contents of the
 1054 nucleon (which are needed to interpret $\mu \rightarrow e$ conversion and dark-matter experiments), and the nucleon
 1055 axial form factor (which enters the determination of the neutrino flux at many accelerator-based neutrino
 1056 experiments). Smaller-scale lattice-QCD calculations of nucleon EDMs, proton- and neutron-decay matrix
 1057 elements, and neutron-antineutron oscillation matrix elements are also in progress. These are very important
 1058 for the intensity frontier as a whole, although not directly relevant to quark-flavor physics.

1059 In the remainder of this subsection, we describe the major new efforts that are underway or envisaged for
 1060 the next 5 or so years, considering in turn kaons, D mesons and B mesons, and close with a 15-year vision.

1061 1.6.1 Future lattice calculations of kaon properties

1062 **$K \rightarrow \pi\pi$ amplitudes:** These amplitudes are now active targets of lattice-QCD calculations. The final-
 1063 state pions can be arranged to have physical, energy-conserving relative momentum by imposing appropriate
 1064 boundary Corrections for the effects of working in finite volume can be made following the analysis of
 1065 Ref. [121]. A first calculation of the amplitude to the $I = 2$ two-pion state, A_2 , has been performed [115]
 1066 with physical kinematics but 15% finite lattice spacing errors. Calculations are now underway using two
 1067 ensembles with smaller lattice spacings which will allow a continuum extrapolation, removing this error.
 1068 Results with an overall systematic error of $\approx 5\%$ are expected within the coming year.

1069 The calculation of A_0 is much more difficult because of the overlap between the $I = 0$ $\pi\pi$ state and the
 1070 vacuum, resulting in disconnected diagrams and a noise to signal ratio that grows exponentially with time
 1071 separation. In addition, for $I = 0$, G -parity boundary conditions must be employed and imposed on both the
 1072 valence and sea quarks. These topics have been actively studied for the past three years [122] and G -parity
 1073 boundary conditions successfully implemented [123]. First results with physical kinematics are expected
 1074 within two years from a relatively coarse, $32^3 \times 64$ ensemble. Errors on ϵ'_K on the order of 15% should be
 1075 achieved, with the dominant error coming from the finite lattice spacing. As in the case of the easier A_2
 1076 calculation, lessons learned from this first, physical calculation will then be applied to calculations using a
 1077 pair of ensembles with two lattice spacings so that a continuum limit can be obtained. A five-year time-frame
 1078 may be realistic for this second phase of the calculation. Essential to the calculation of both A_0 and A_2 is the
 1079 renormalization of the lattice operators. Significant efforts will be required in the next 2-3 years to extend
 1080 the range of nonperturbative renormalization methods up through the charm threshold and to a scale of 4-5
 1081 GeV where perturbative matching to the conventional $\overline{\text{MS}}$ scheme will have small and controlled errors.

1082 **Long-distance contributions to Δm_K and ϵ_K :** Promising techniques have been developed which allow
 1083 the calculation of the long-distance contribution to kaon mixing by lattice methods. By evaluating a four-
 1084 point function including operators which create and destroy the initial and final kaons and two effective weak
 1085 four-quark operators, the required second order amplitude can be explicitly evaluated. Integrating the space-
 1086 time positions of the two weak operators over a region of fixed time extent T and extracting the coefficient
 1087 of the term which grows linearly with T gives precisely both Δm_K and ϵ_K . This Euclidean space treatment
 1088 of such a second-order process contains unphysical contributions which grow exponentially with T and must
 1089 be subtracted. The statistical noise remaining after this subtraction gives even the connected diagrams
 1090 the large-noise problems typical of disconnected diagrams. Preliminary results suggest that this problem
 1091 can be solved by variance reduction methods and large statistics [120]. Given the central importance of
 1092 GIM cancellation in neutral kaon mixing, a lattice calculation that is not burdened by multiple subtractions
 1093 must include the charm quark mass with consequent demands that the lattice spacing be small compared to
 1094 $1/m_c$ — a substantial challenge for a calculation which should also contain physical pions in an appropriately

1095 large volume. Perturbative results [124] as well as the first lattice calculation [120] suggest that perturbation
 1096 theory works poorly at energies as low as the charm mass, making the incorporation of charm in a lattice
 1097 calculation a high priority. Given the challenge of including both physical pions and active charm quarks,
 1098 the first calculation of Δm_K may take 4–5 years. Results for the long-distance part of ϵ_K may be obtained
 1099 in a similar time frame. However, a more challenging subtraction procedure must be employed for ϵ_K .

1100 **Rare kaon decays:** Given the promise of the first calculations of the long distance contributions to Δm_K ,
 1101 a process that involves two W^\pm exchanges, it is natural to consider similar calculations for the second-
 1102 order processes which enter important rare kaon decays such as $K_L^0 \rightarrow \pi^0 \ell^+ \ell^-$ and $K^+ \rightarrow \pi^+ \nu \bar{\nu}$. While
 1103 in principle $K_L \rightarrow \ell^+ \ell^-$ should also be accessible to lattice methods, the appearance of three electroweak,
 1104 hadronic vertices suggests that this and similar processes involving $H_W^{\Delta S=1}$ and two photons, should be
 1105 tackled only after success has been achieved with more accessible, second order processes.

1106 The processes $K^+ \rightarrow \pi^+ \nu \bar{\nu}$ and $K_L \rightarrow \pi^0 \nu \bar{\nu}$ may be the most straightforward generalization of the current
 1107 Δm_K calculation. Here the dominant contribution comes from box and Z -penguin diagrams involving top
 1108 quarks, but with a 30% component of the CP-conserving process coming from the charm quark [125]. While
 1109 the charm quark piece is traditionally referred to as “short distance,” the experience with Δm_K described
 1110 above suggests that a nonperturbative evaluation of this charm-quark contribution may be a necessary check
 1111 of the usual perturbative approach, which is here believed to be reliable. There are also “longer distance”
 1112 contributions which are only accessible to lattice methods and will become important when the accuracy of
 1113 rare kaon decay experiments reaches the 3% level, or possibly sooner. The long-distance contributions to
 1114 the decay $K_{L/S} \rightarrow \pi^0 \ell^+ \ell^-$ also appear to be a natural target for a lattice-QCD calculation since the sign of
 1115 the CP-conserving process $K_S \rightarrow \pi^0 \ell^+ \ell^-$ may be only determined this way.

1116 1.6.2 Future lattice calculations of D -meson properties

1117 **$D \rightarrow \pi\pi$, KK amplitudes:** Recent experimental evidence suggests that there may be CP violation in
 1118 $D \rightarrow \pi\pi$ and $D \rightarrow KK$ decays. In order to interpret these results, it is essential to be able to predict the CP
 1119 violation expected in the SM. Even a result with a large, but reliable, error could have a large impact. This
 1120 need will become even more acute over the next five years as LHCb and Belle II improve the measurements.

1121 This calculation is more challenging than that for $K \rightarrow \pi\pi$ decays, which represent the present frontier of
 1122 lattice calculations. In the kaon case, one must deal with the fact that two-pion states in finite volume are
 1123 not asymptotic states, and the presence of multiple quark-disconnected contractions. For D decays, even
 1124 when one has fixed the strong-interaction quantum numbers of a final state (say to $I = S = 0$), the strong
 1125 interactions necessarily bring in multiple final states: $\pi\pi$ and $K\bar{K}$ mix with $\eta\eta$, 4π , 6π , etc. The finite-
 1126 volume states used by lattice QCD are inevitably mixtures of all these possibilities, and one must learn how,
 1127 in principle and in practice, to disentangle these states to obtain the desired matrix element. Recently, a
 1128 first step towards developing a complete method has been taken [126], in which the problem has been solved
 1129 in principle for any number of two-particle channels, and assuming that the scattering is dominantly S wave.
 1130 This is encouraging, and this method may allow one to obtain semi-quantitative results for the amplitudes of
 1131 interest. We expect that turning this method into practice will take ~ 5 years due to a number of numerical
 1132 challenges (in particular the need to calculate several energy levels with good accuracy).

1133 In the more distant future, we expect that it will be possible to generalize the methodology to include four-
 1134 particle states; several groups are actively working on the theoretical issues and much progress has been
 1135 made already for three particles.

1136 **$D - \bar{D}$ mixing:** Mixing occurs in the $D^0 - \bar{D}^0$ system, and there is no evidence yet for CP violation in
 1137 this mixing [61]. The short-distance contributions can be calculated for D mesons using lattice QCD, as
 1138 for kaons and B mesons. The challenge, however, is to calculate the long-distance contributions. As in
 1139 the case of Δm_K discussed above, there are two insertions of the weak Hamiltonian, with many allowed
 1140 states propagating between them. The D system is much more challenging, however, since, as for the decay
 1141 amplitudes, there are many strong-interaction channels having $E < m_D$. Further theoretical work is needed
 1142 to develop a practical method.

1143 1.6.3 Future lattice calculations of B -meson properties

1144 **$B \rightarrow D^{(*)}\ell\nu$ form factors at nonzero recoil:** Lattice-QCD results for these form factors allow for the
 1145 determination of $|V_{cb}|$ from the measured decay rates. For the $B \rightarrow D^*\ell\nu$ form factor at zero recoil, the gap
 1146 between experimental errors (1.3%) and lattice errors (currently $\sim 1.8\%$) has narrowed considerably over
 1147 the last five years. In the next five years, we expect the lattice contribution to the error in $|V_{cb}|$ to drop
 1148 below the experimental one, as shown in Table 1-6. Particularly important for this will be the extension of
 1149 the $B \rightarrow D^{(*)}\ell\nu$ form-factor calculations to nonzero recoil [127].

1150 **Tauonic B -decay matrix elements:** Recently the *BABAR* collaboration measured the ratios $R(D^{(*)}) =$
 1151 $\mathcal{B}(B \rightarrow D^{(*)}\tau\nu)/\mathcal{B}(B \rightarrow D^{(*)}\ell\nu)$ with $\ell = e$ or μ , and observed a combined excess over the existing SM
 1152 predictions of 3.4σ [128]. Those SM predictions were based, however, on models of QCD, not *ab initio*
 1153 QCD. Realizing that it was much easier to obtain accurate results for these ratios than for the form factors
 1154 themselves, the Fermilab-MILC collaboration responded quickly (using lattice data already in hand), and
 1155 provided the first lattice-QCD result for $R(D)$ [129]. Their result slightly reduced the discrepancy with
 1156 experiment for $R(D)$ from $2.0 \rightarrow 1.7\sigma$. At present, the experimental errors in $R(D)$ ($\sim 16\%$) dominate over
 1157 lattice errors (4.3%), so further lattice improvements are not needed in the short run. The experimental
 1158 uncertainties will shrink with the increased statistics available at Belle II, and it should be straightforward
 1159 to reduce the corresponding lattice-QCD error by a factor of two over the next five years. Work is also in
 1160 progress to calculate $R(D^*)$, for which the uncertainties are expected to be comparable to those of $R(D)$.

1161 Belle II will also reduce the uncertainty in the experimental measurement of $\mathcal{B}(B \rightarrow \tau\nu)$ to the few-percent
 1162 level with its anticipated full data set. In the next five years, lattice-QCD calculations are expected to reduce
 1163 the error in f_B to the percent level (see Table 1-6). Particularly important for this will be the use of finer
 1164 lattice spacings that permit relativistic b -quark actions [130]. Combined with the anticipated experimental
 1165 precision, this will increase the reach of new-physics searches in $B \rightarrow \tau\nu$; moreover, correlations between
 1166 $B \rightarrow \tau\nu$ and $B \rightarrow D^{(*)}\tau\nu$ decays can help distinguish between new-physics models.

1167 **$B \rightarrow K\ell^+\ell^-$ and related decay form factors:** The branching ratio for $B \rightarrow K\ell^+\ell^-$ is now well mea-
 1168 sured, and increasingly accurate results from LHCb, and eventually Belle II, are expected. The SM prediction
 1169 requires knowledge of the vector and tensor $b \rightarrow s$ form factors across the kinematic range. Present
 1170 theoretical estimates use light-cone sum rules, but several first-principles lattice-QCD calculations are nearing
 1171 completion, as reviewed in Ref. [131]. The calculation is similar to that needed for the $B \rightarrow \pi\ell\nu$ form factor,
 1172 and we expect similar accuracy to be obtained over the next five years.

1173 A related process is the baryonic decay $\Lambda_b \rightarrow \Lambda\ell^+\ell^-$, recently measured by CDF. Here the extra spin degree
 1174 of freedom can more easily distinguish between SM and BSM contributions. A lattice-QCD calculation of
 1175 the required form factors has recently been completed, using HQET to describe the b quark [132]. Errors of
 1176 $\sim 10\text{--}15\%$ in the form factors are obtained, which are comparable to present experimental errors. The latter
 1177 errors will decrease with new results from LHCb, and so improved LQCD calculations and cross-checks are

1178 needed. Although the calculation is conceptually similar to that for $B \rightarrow K\ell^+\ell^-$, given the presence of
 1179 baryons we expect the errors for $\Lambda_b \rightarrow \Lambda\ell^+\ell^-$ to lag somewhat behind.

1180 **Non-standard model form factors for $K \rightarrow \pi$ and $B \rightarrow \pi$ transitions:** The $B \rightarrow K$ vector and
 1181 tensor form factors just discussed are also needed to describe decays involving missing energy, $B \rightarrow KX$, in
 1182 BSM theories [33]. Analogous form factors are needed for $B \rightarrow \pi X$ and $K \rightarrow \pi X$ decays. The tensor form
 1183 factors are also needed to evaluate some BSM contributions to $K \rightarrow \pi\ell^+\ell^-$ [133]. Thus it is of interest to
 1184 extend the present calculations of vector form factors in $K \rightarrow \pi$ and $B \rightarrow \pi$ to include the tensor matrix
 1185 elements. Since these are straightforward generalizations of present calculations, we expect that comparable
 1186 accuracy to the present errors in Table 1-6 can be obtained quickly, and that future errors will continue to
 1187 follow the projections for similar matrix elements.

1188 1.6.4 Lattice QCD and flavor physics: 2018–2030

1189 The discussion above has laid out an ambitious vision for future lattice-QCD calculations on a five-year
 1190 timescale, explaining how they can provide essential and timely information for upcoming quark-flavor
 1191 experiments. Also discussed are a number of more challenging quantities which have become accessible to
 1192 lattice methods only recently. In this section we discuss more generally the opportunities offered by lattice
 1193 methods over the extended time period covered by the Snowmass study. However, we should emphasize
 1194 that these longer range forecasts are made difficult by the very rapid evolution of this emerging field, which
 1195 is driven by both rapidly advancing commercial computer technology and continual, difficult-to-anticipate
 1196 advances in algorithms.

1197 We begin with the conservative assumptions that exascale performance (10^{18} floating point operations/second)
 1198 will be achieved by 2020, and that a further factor of 100 will be available by 2030. These represent factors
 1199 of 10^2 and 10^4 over presently available capability. At fixed physical quark masses, the difficulty of modern
 1200 lattice-QCD algorithms scales with decreasing lattice spacing a as $1/a^6$ and with increasing physical linear
 1201 problem size L as L^5 . Present large-scale lattice calculations at physical quark masses are performed in
 1202 volumes of linear size $L \approx 6$ fm and with inverse lattice spacing $1/a$ as small as ~ 2.5 GeV. Thus, these 10^2
 1203 and 10^4 advances in computer capability will allow an increase in physical volume to 15 and 36 fm and in
 1204 inverse lattice spacing to 5 and 10 GeV, respectively. Statistical errors can be reduced from their present
 1205 percent-level for many quantities to 0.1% or even 0.01% as needed.

1206 These three directions of substantial increase in capability translate directly into physics opportunities. The
 1207 large increase in possible Monte Carlo statistics is necessary if we are to decrease the errors on many of the
 1208 quantities in Table 1-6 to the 0.1% level. Such increased statistics will also directly support perhaps 1%
 1209 precision for results that depend on disconnected diagrams such as ϵ'_K and the $K_L - K_S$ mass difference.
 1210 For most QCD calculations, the non-zero pion mass implies that finite volume effects decrease exponentially
 1211 in the linear size of the system. However, this situation changes dramatically when electromagnetic effects
 1212 are included. Here the massless photon and related difficulties of dealing with charged systems in finite
 1213 volume result in substantial finite volume errors which decrease only as a power of L as the linear system
 1214 size L becomes large. The ability to work on systems of linear size 20 or 30 fm will play an important role
 1215 in both better understanding electromagnetic effects using lattice methods and achieving the 10% errors in
 1216 the computation of such effects that are needed to attain 0.1% errors in many of the quantities in Table 1-6.

1217 Finally the ability to work with an inverse lattice spacing as large as 10 GeV will allow substantial improve-
 1218 ments in the treatment of heavy quarks. Using $3 \text{ GeV} \leq 1/a \leq 5 \text{ GeV}$, calculations involving charm quarks
 1219 will have controlled finite lattice spacing errors on the 1% level or smaller. As a result calculation of the
 1220 long-distance contributions, up to and including the charm scale, will be possible for Δm_K , ϵ_K and rare kaon

1221 decays yielding errors of order 1% for these important quantities. The larger inverse lattice spacings in the
 1222 range $6 \text{ GeV} \leq 1/a \leq 10 \text{ GeV}$ will allow the present estimates of the finite lattice spacing errors in bottom
 1223 quark systems to both be substantially reduced and to be refined using the new information provided by a
 1224 larger range of lattice spacings. This will allow many quantities involving bottom quarks to be determined
 1225 with errors well below 1%.

1226 While ever more difficult to forecast, a 10^4 increase in capability can be expected to significantly expand
 1227 the range of quantities that can be computed using lattice methods. These include the $D - \bar{D}$ mixing and
 1228 multi-particle D decays discussed in the previous section as well as even more challenging quantities such
 1229 as semileptonic B decays with vector mesons in the final state. These are relevant both for the extraction
 1230 of CKM matrix elements (e.g., $B \rightarrow \rho \ell \nu$ provides an alternative determination of $|V_{ub}|$) and new-physics
 1231 searches (e.g., measurements of $B \rightarrow K^* \ell^+ \ell^-$, $B \rightarrow K^* \gamma$ and $B_s \rightarrow \phi \gamma$ probe $b \rightarrow s$ flavor-changing neutral
 1232 currents). A second example is nonleptonic B decays, such as $B \rightarrow D\pi(K)$, which can be used to obtain the
 1233 CKM angle γ .

1234 Clearly an enhanced computational capability of four orders of magnitude, coupled with possibly equally
 1235 large advances in numerical algorithms, will have a dramatic effect on the phenomena that can be analyzed
 1236 and precision that can be achieved using lattice methods. The possibility of making SM predictions with
 1237 errors which are an order of magnitude smaller than present experimental errors will create an exciting
 1238 challenge to identify quantities where substantially increased experimental accuracy is possible and where
 1239 the impact of such measurements on the search for physics beyond the SM most sensitive. With the ability
 1240 to make highly accurate SM predictions for a growing range of quantities, experiments can be designed
 1241 that will achieve the greatest precision for quantities sensitive to physics beyond the SM, rather than being
 1242 limited to those quantities which are least obscured by the effects of QCD.

1243 1.7 A U.S. Plan for Quark Flavor Physics

1244 Until recently, the U.S. had onshore accelerator facilities that supported a leadership role at both the Energy
 1245 and Intensity Frontiers. With the successful start of the LHC and the termination of the Tevatron program,
 1246 the Energy Frontier has migrated offshore for the foreseeable future. With choices summarized in Section 1.1,
 1247 the U.S. ceded leadership in much of quark-flavor physics. It is difficult to foresee a scenario that leads to the
 1248 construction of a facility in the U.S. that is capable of supporting B -physics or charm-physics experiments
 1249 during the current decade or even the next decade. Indeed, the only accelerator-based experiments currently
 1250 in the DOE pipeline are neutrino experiments and muon experiments at Fermilab, and to achieve their full
 1251 potential these experiments depend on Fermilab's Project-X facility, which has yet to achieve the first level
 1252 of DOE approval ("mission need"). It is under these rather dire circumstances, facing the prospect that
 1253 the U.S. accelerator-based HEP program may go the way of the dodo bird, that we must contemplate the
 1254 question of whether and how the U.S. should pursue research in quark-flavor physics.

1255 There is a strong physics case for quark-flavor physics that remains robust in all LHC scenarios. It rests,
 1256 quite simply, on the potential of precision quark-flavor experiments and studies of very rare decays to observe
 1257 the effect of high-mass virtual particles. If new physics is observed at LHC, tighter constraints from the
 1258 flavor sector will narrow the range of models that can account for the observed states. If new physics is not
 1259 discovered at LHC, then the reach to mass scales beyond that of LHC will still offer the potential to find new
 1260 physics and to estimate the scale needed for direct observation. International recognition of the importance
 1261 of quark-flavor physics is evident from the commitments in Europe and Asia to conduct the next-generation
 1262 of B -physics, charm, and kaon experiments.

1263 In the U.S., the goal should be to construct an HEP program that has the breadth to assure meaningful
1264 participation in making the discoveries that will define the future of this field. The successful U.S. contri-
1265 butions to LHC have demonstrated that physicists from U.S. laboratories and universities can play essential
1266 roles in offshore experiments. If this paradigm works at the Energy Frontier, it can work at the Intensity
1267 Frontier as well. Therefore, significant U.S. contributions to offshore quark-flavor experiments such as LHCb
1268 and Belle II should be encouraged. Also, in the one area where existing and foreseeable facilities on U.S.
1269 soil can support a world-leading program — kaon physics — the U.S. should embrace the opportunity. The
1270 accelerator facilities required for kaon experiments are exactly those needed for the neutrino program, so
1271 the costs are incremental and relatively modest. Below, we summarize the opportunities that exist now and
1272 those that will exist during the next decade.

1273 1.7.1 Opportunities in This Decade

1274 The Task Force reports have described current, planned, and possible B -physics, charm, and kaon experi-
1275 ments in Europe and Asia. There is a strong and diverse international program. The only U.S. entry in the
1276 discussion of the immediate future for quark-flavor physics experiments is the ORKA proposal at Fermilab,
1277 for an experiment which would make a precise measurement of the $K^+ \rightarrow \pi^+ \nu \bar{\nu}$ branching fraction.

1278 For the remainder of this decade, the plans in Europe and Asia appear to be set, and the experiments there
1279 (those already running or under construction) will define the frontier of quark-flavor physics. These are
1280 LHCb and NA62 at CERN, KLOE2 in Italy, Panda in Germany, BESIII in China, and Belle II, KOTO, and
1281 TREK in Japan. This is a rich program, and fortunately U.S. physicists have some involvement in most
1282 of them. While all of these experiments have important physics goals and capabilities, the scale of LHCb
1283 and Belle II, and their incredibly broad physics menus including both bottom and charm, means that they
1284 will be the flagship experiments in quark-flavor physics. In view of that, the U.S. role in these experiments
1285 should be significant.

1286 The outstanding question is whether the ORKA experiment will go forward at Fermilab. It received “Stage 1”
1287 approval from Fermilab in the fall of 2011, but has not been integrated into DOE’s planned program thus
1288 far. A clear conclusion of this working group is that ORKA presents an extraordinary opportunity. If the
1289 U.S. HEP program endeavors to achieve a leading role at the Intensity Frontier, ORKA should be pursued.

1290 In short, the optimal U.S. plan in quark-flavor physics for the remainder of this decade has four elements.

- 1291 • U.S. physicists should be supported to carry out significant roles in LHCb and Belle II.
- 1292 • The ORKA experiment should move forward in a timely way at Fermilab.
- 1293 • Support for U.S participation on other experiments that are in progress (e.g., KOTO, TREK, BESIII)
1294 should be maintained.
- 1295 • Support for theory, and the computing facilities needed for progress in Lattice QCD, should be
1296 maintained.

1297 1.7.2 Opportunities in the Next Decade

1298 In the decade beginning around 2020, we can anticipate that LHCb will be well on its path toward collecting
1299 50 fb^{-1} and Belle II will be well on its path toward 50 ab^{-1} . These will be very complementary data samples,

1300 overlapping in some areas but providing different strengths in others. We cannot, of course, predict what
1301 the LHC experiments may have found by then, nor what surprising results may have come from any of the
1302 quark-flavor experiments discussed above. Based on what is learned between now and then, new priorities
1303 and new experimental directions may emerge.

1304 Nonetheless, we anticipate that the U.S. HEP program will be continuing its emphasis on Intensity Frontier
1305 experiments, with a commitment to providing high-intensity proton sources for the production of neutrino
1306 beams for neutrino experiments. If so, the potential for such a high-intensity proton source to support the
1307 next generation of rare kaon decay experiments is an opportunity unique to the U.S. program. In particular,
1308 Project-X at Fermilab can deliver more than an order of magnitude increase in the beam power available
1309 for producing kaons compared to any other laboratory in the world. In addition, the CW-linac of Project-X
1310 can provide a time structure that is programmable bunch-by-bunch. That capability can be exploited in
1311 neutral kaon experiments to measure the momentum of individual K_L^0 's via time-of-flight, opening the door
1312 to dramatic improvements in background rejection for some challenging rare decays.

1313 Project-X can be the leading facility in the world for rare kaon decay experiments.

1314 1.7.3 Conclusions

1315 This report has described the physics case for precision studies of flavor-changing interactions of bottom,
1316 charm, and strange quarks, and it has described the experimental programs that are underway and foreseeable
1317 around the world. A substantial number of physicists in the U.S. are motivated to work in this area, both
1318 theorists and experimentalists. Quark-flavor physics should be a component in the plan for the future U.S.
1319 HEP program.

1320 After enduring the full “Snowmass process,” the Quark Flavor Physics working group has produced this
1321 report. It reflects a wide range of inputs. Its contents and conclusions have been publicly vetted. For
1322 instance, drafts of this report were posted for two rounds of public comment.

1323 Our major conclusions can be summarized as follows:

- 1324 • Quark flavor physics is an essential element in the international high-energy physics program. Exper-
1325 iments that study the properties of highly suppressed decays of strange, charm, and bottom quarks
1326 have the potential to observe signatures of new physics at mass scales well beyond those accessible by
1327 current or foreseeable accelerators.
- 1328 • The importance of quark flavor physics is recognized in Europe and Asia, as demonstrated by the
1329 commitments to LHCb, NA62, KLOE-2, and Panda in Europe, and to Belle-II, BES-III, KOTO, and
1330 TREK in Asia.
- 1331 • In order for the U.S. HEP program to have the breadth to assure meaningful participation in future
1332 discoveries, significant U.S. contributions to offshore quark-flavor experiments is important. In par-
1333 ticular, U.S. contributions to LHCb and Belle II should be encouraged because of the richness of the
1334 physics menus of these experiments and their reach for new physics.
- 1335 • Existing facilities at Fermilab are capable of mounting world-leading rare kaon decay experiments in
1336 this decade at modest incremental cost to running the Fermilab neutrino program. The proposed
1337 ORKA experiment, to measure the rare decay $K^+ \rightarrow \pi^+ \nu \bar{\nu}$ with high precision, provides such an
1338 opportunity. This is a compelling opportunity that should be exploited.

- 1339
- 1340
- 1341
- 1342
- Longer term, Project-X at Fermilab can become the dominant facility in the world for rare kaon decay experiments. Its potential to provide ultra-high intensity kaon beams with tunable time structure is unprecedented. While the physics case for Project-X is much broader than its capabilities for kaon experiments, the power of a Project-X kaon program is a strong argument in its favor.
- 1343
- Back-and-forth between theory and experiment is necessary for progress in quark-flavor physics, as in any field of physics. Therefore, stable support for theorists working in this area is essential. Lattice QCD plays a crucial role, and support for the computing facilities needed for LQCD progress should be maintained.
- 1344
- 1345
- 1346

1347 Quark flavor physics will be the source of future discoveries. A healthy U.S. particle physics program will
1348 endeavor to be among the leaders in this research.

DRAFT

References

- [1] J. L. Hewett *et al.*, arXiv:1205.2671 [hep-ex].
- [2] M. Kobayashi and T. Maskawa, Prog. Theor. Phys. **49**, 652 (1973).
- [3] N. Cabibbo, Phys. Rev. Lett. **10**, 531 (1963).
- [4] S.L. Glashow, J. Iliopoulos, and L. Maiani, Phys. Rev. D **2**, 1285 (1970).
- [5] M.K. Gaillard and B.W. Lee, Phys. Rev. D **10**, 897 (1974).
- [6] A.I. Vainshtein and I.B. Khriplovich, Pisma Zh. Eksp. Theor. Fiz. **18**, 141 (1973) [JETP Lett. **18**, 83 (1973)].
- [7] G. Isidori, Y. Nir and G. Perez, Ann. Rev. Nucl. Part. Sci. **60**, 355 (2010) [arXiv:1002.0900 [hep-ph]]; and updates in G. Isidori, arXiv:1302.0661 [hep-ph].
- [8] A. Höcker, H. Lacker, S. Laplace and F. Le Diberder, Eur. Phys. J. C **21**, 225 (2001) [hep-ph/0104062]; and updates at <http://ckmfitter.in2p3.fr/>.
- [9] J. Charles *et al.*, Eur. Phys. J. C **41**, 1 (2005) [hep-ph/0406184].
- [10] L. Wolfenstein, Phys. Rev. Lett. **51**, 1945 (1983).
- [11] A. Hocker and Z. Ligeti, Ann. Rev. Nucl. Part. Sci. **56**, 501 (2006) [hep-ph/0605217].
- [12] Z. Ligeti, Int. J. Mod. Phys. A **20**, 5105 (2005) [hep-ph/0408267].
- [13] M. Bona *et al.* [UTfit Collaboration], JHEP **0803**, 049 (2008) [arXiv:0707.0636]; and updates at <http://utfit.org/>.
- [14] A. Lenz *et al.*, Phys. Rev. D **86** (2012) 033008 [arXiv:1203.0238 [hep-ph]].
- [15] Y. Grossman, Z. Ligeti and Y. Nir, Prog. Theor. Phys. **122**, 125 (2009) [arXiv:0904.4262 [hep-ph]].
- [16] J. Brod, contribution to “Kaon Physics with Project X”, in Ref. [17].
- [17] A. S. Kronfeld *et al.*, arXiv:1306.5009 [hep-ex].
- [18] S. Jäger, talk given at the NA62 Physics Handbook Workshop, <http://indico.cern.ch/get-File.py/access?contribId=5&resId=0&materialId=slides&confId=65927>
- [19] A. J. Buras, P. Gambino, M. Gorbahn, S. Jäger and L. Silvestrini, Nucl. Phys. B **592**, 55 (2001) [hep-ph/0007313].
- [20] M. Bauer, S. Casagrande, U. Haisch and M. Neubert, JHEP **1009**, 017 (2010) [arXiv:0912.1625 [hep-ph]].
- [21] M. Blanke, A. J. Buras, S. Recksiegel, C. Tarantino and S. Uhlig, JHEP **0706**, 082 (2007) [arXiv:0704.3329 [hep-ph]].
- [22] A. J. Buras and L. Silvestrini, Nucl. Phys. B **546**, 299 (1999) [hep-ph/9811471].
- [23] A. J. Buras, G. Colangelo, G. Isidori, A. Romanino and L. Silvestrini, Nucl. Phys. B **566**, 3 (2000) [hep-ph/9908371].
- [24] U. Haisch, contribution to “Kaon Physics with Project X”, in Ref. [17].
- [25] S. Adler *et al.* (E949 & E787 Collaborations), Phys. Rev. D **77**:052003 (2008) [arXiv:0709.1000]
- [26] Y. Grossman and Y. Nir, Phys. Lett. B **398**, 163 (1997) [hep-ph/9701313].
- [27] M. Blanke, Acta Phys. Polon. B **41**, 127 (2010), [arXiv:0904.2528]
- [28] F. Mescia, C. Smith and S. Trine, JHEP **0608**, 088 (2006) [hep-ph/0606081].

- 1387 [29] M. Blanke, A. J. Buras, B. Duling, K. Gemmler and S. Gori, JHEP **0903**, 108 (2009) [arXiv:0812.3803
1388 [hep-ph]].
- 1389 [30] M. Blanke, A. J. Buras, B. Duling, S. Recksiegel, and C. Tarantino, Acta Phys. Polon B **41**, 657 (2010)
1390 [arXiv:0906.5454 [hep-ph]].
- 1391 [31] A. J. Buras, F. De Fazio and J. Girrbach, JHEP **1302**, 116 (2013) [arXiv:1211.1896 [hep-ph]].
- 1392 [32] A. J. Buras, T. Ewerth, S. Jäger and J. Rosiek, Nucl. Phys. B **714**, 103 (2005) [hep-ph/0408142].
- 1393 [33] J. F. Kamenik and C. Smith, JHEP **1203**, 090 (2012) [arXiv:1111.6402 [hep-ph]].
- 1394 [34] V. Cirigliano and I. Rosell, Phys. Rev. Lett. **99**, 231801 (2007) [arXiv:0707.3439 [hep-ph]].
- 1395 [35] V. P. Efrosinin, I. B. Khriplovich, G. G. Kirilin and Y. G. Kudenko, Phys. Lett. B **493**, 293 (2000)
1396 [hep-ph/0008199].
- 1397 [36] <http://na62.web.cern.ch/na62/Documents/ReferenceDocuments.html>.
- 1398 [37] <http://koto.kek.jp/>.
- 1399 [38] <http://trek.kek.jp/>.
- 1400 [39] <http://www.lnf.infn.it/kloe2/>.
- 1401 [40] J. Comfort *et al.*, FERMILAB-PROPOSAL-1021 (2011).
- 1402 [41] KOPIO Experiment Proposal (2005), <http://www.bnl.gov/rsvp/KOPIO.htm>.
- 1403 [42] Lattice QCD at the intensity frontier, T. Blum *et al.* [USQCD Collaboration], available at <http://www.usqcd.org/documents/13flavor.pdf>.
- 1404 [43] J. Zupan, arXiv:1101.0134 [hep-ph].
- 1405 [44] R. Aaij *et al.* [LHCb Collaboration], arXiv:1304.2600 [hep-ex].
- 1406 [45] R. Aaij *et al.* [LHCb Collaboration], Phys. Rev. Lett. **110** (2013) 021801 [arXiv:1211.2674 [hep-ex]].
- 1407 [46] A. J. Buras, J. Girrbach, D. Guadagnoli and G. Isidori, Eur. Phys. J. C **72** (2012) 2172 [arXiv:1208.0934
1408 [hep-ph]].
- 1409 [47] K. De Bruyn *et al.*, Phys. Rev. Lett. **109**, 041801 (2012) [arXiv:1204.1737].
- 1410 [48] S. Chatrchyan *et al.* [CMS Collaboration], arXiv:1307.5025 [hep-ex], submitted to Phys. Rev. Lett.
- 1411 [49] A. Aaij *et al.* [LHCb Collaboration], arXiv:1307.5024 [hep-ex], submitted to Phys. Rev. Lett.
- 1412 [50] V. M. Abazov *et al.* [D0 Collaboration], Phys. Rev. D **84** (2011) 052007 [arXiv:1106.6308 [hep-ex]].
- 1413 [51] S. Laplace, Z. Ligeti, Y. Nir and G. Perez, Phys. Rev. D **65** (2002) 094040 [hep-ph/0202010].
- 1414 [52] Z. Xing *et al.* [LHCb Collaboration], arXiv:1212.1175 [hep-ex].
- 1415 [53] J. P. Lees *et al.* [BaBar Collaboration], arXiv:1303.0571 [hep-ex].
- 1416 [54] S. Fajfer, J. F. Kamenik, I. Nisandzic and J. Zupan, Phys. Rev. Lett. **109**, 161801 (2012)
1417 [arXiv:1206.1872 [hep-ph]].
- 1418 [55] T. Aushev *et al.* [Belle II Collaboration], arXiv:1002.5012 [hep-ex].
- 1419 [56] M. Bona *et al.* [SuperB Collaboration], [arXiv:0709.0451 [hep-ex]].
- 1420 [57] I. Adachi *et al.* [Belle Collaboration], Phys. Rev. Lett. **108** (2012) 171802 [arXiv:1201.4643 [hep-ex]].
- 1421 [58] B. Aubert *et al.* [BaBar Collaboration], Phys. Rev. D **79** (2009) 072009 [arXiv:0902.1708 [hep-ph]].
- 1422 [59] H. Ishino *et al.* [Belle Collaboration], Phys. Rev. Lett. **98** (2007) 211801 [arXiv:hep-ex/0608035].
- 1423 [60] J. P. Lees *et al.* [BaBar Collaboration], Phys. Rev. D **87** (2012) 052009 [arXiv:1206.3525 [hep-ph]].
- 1424 [61] J. Beringer *et al.* [Particle Data Group Collaboration], Phys. Rev. D **86**, 010001 (2012).
1425

- 1426 [62] Y. Amhis *et al.* [Heavy Flavor Averaging Group], [arXiv:1207.1158 [hep-ex]], and updates at <http://www.slac.stanford.edu/xorg/hfag/>.
1427
- 1428 [63] M. Gronau, Phys. Lett. B **627** (2005) 82 [arXiv:hep-ph/0508047].
- 1429 [64] M. Fujikawa *et al.* [Belle Collaboration], Phys. Rev. D **81** (2010) 011101 [arXiv:0809.4366 [hep-ex]].
- 1430 [65] J. Charles *et al.* [CKM Fitter Group], Phys. Rev. D **84** (2011) 033005 [arXiv:1106.4041 [hep-ph]].
- 1431 [66] B. Aubert *et al.* [BaBar Collaboration], Phys. Rev. D **81** (2010) 051101 [arXiv:0912.2453 [hep-ex]].
- 1432 [67] K. Hara *et al.* [Belle Collaboration], Phys. Rev. D **82** (2010) 071101 [arXiv:1006.4201 [hep-ex]].
- 1433 [68] J. P. Lees *et al.* [BaBar Collaboration], [arXiv:1207.0698 [hep-ex]].
- 1434 [69] I. Adachi *et al.* [Belle Collaboration], Phys. Rev. Lett. **110** (2013) 131801 [arXiv:1208.4678 [hep-ex]].
- 1435 [70] CDF B -physics results may be found at <http://www-cdf.fnal.gov/physics/new/bottom/bottom.html>.
1436
- 1437 [71] DO B -physics results may be found at <http://www-d0.fnal.gov/Run2Physics/WWW/results/b.htm>.
- 1438 [72] A. A. Alves, Jr. *et al.* [LHCb Collaboration], JINST **3**, S08005 (2008).
- 1439 [73] R. Aaij *et al.*, JINST **8**, P04022 (2013) [arXiv:1211.3055 [hep-ex]].
- 1440 [74] R. Aaij *et al.* [LHCb Collaboration], LHCb-PUB-2012-006, Eur. Phys. J. C **73**, 2373 (2013)
1441 [arXiv:1208.3355 [hep-ex]]; See also a summary in LHCb-PUB-2012-009.
- 1442 [75] I. Bediaga *et al.* [LHCb Collaboration] CERN-LHCC-2012-007 ; LHCb-TDR-12.
- 1443 [76] S. Stone and L. Zhang, Phys. Rev. D **79**, 074024 (2009) [arXiv:0812.2832 [hep-ph]].
- 1444 [77] R. Aaij *et al.* [LHCb Collaboration], Phys. Rev. D **86**, 052006 (2012) [arXiv:1204.5643 [hep-ex]].
- 1445 [78] S. Chatrchyan *et al.* [CMS Collaboration], JHEP **1204**, 033 (2012) [arXiv:1203.3976 [hep-ex]].
- 1446 [79] G. Aad *et al.* [ATLAS Collaboration], Phys. Lett. B **713**, 387 (2012) [arXiv:1204.0735 [hep-ex]].
- 1447 [80] D. M. Straub, arXiv:1205.6094 [hep-ph].
- 1448 [81] R. Aaij *et al.* [LHCb Collaboration], arXiv:1304.6325 [hep-ex].
- 1449 [82] [CMS Collaboration], CMS-PAS-BPH-11-009, 2013.
- 1450 [83] [ATLAS Collaboration], ATLAS-CONF-2013-038, 2013.
- 1451 [84] R. Aaij *et al.* [LHCb Collaboration], Phys. Rev. Lett. **110**, **241802** (2013) [arXiv:1303.7125 [hep-ex]].
- 1452 [85] R. Aaij *et al.* [LHCb Collaboration], JHEP **1206**, 058 (2012) [arXiv:1204.1620 [hep-ex]].
- 1453 [86] R. Aaij *et al.* [LHCb Collaboration], JHEP **1206**, 141 (2012) [arXiv:1205.0975 [hep-ex]].
- 1454 [87] R. Aaij *et al.* [LHCb Collaboration], Phys. Rev. D **85**, 091103 (2012) [arXiv:1202.5087 [hep-ex]].
- 1455 [88] R. Aaij *et al.* [LHCb Collaboration], Phys. Rev. Lett. **110**, **222001** (2013) [arXiv:1302.6269 [hep-ex]].
- 1456 [89] R. Aaij *et al.* [LHCb Collaboration], Phys. Rev. D **85**, 112004 (2012) [arXiv:1201.5600 [hep-ex]].
- 1457 [90] R. Aaij *et al.* [LHCb Collaboration], Phys. Lett. B **724** (2013) [arXiv:1304.4518 [hep-ex]].
- 1458 [91] V. A. M. Heijne *et al.* [LHCb Collaboration], LHCb-CONF-2012-014, Frascati Phys. Ser. **56**, 162 (2012).
- 1459 [92] D. M. Asner, T. Barnes, J. M. Bian, I. I. Bigi, N. Brambilla, I. R. Boyko, V. Bytev and K. T. Chao *et al.*, Int. J. Mod. Phys. A **24**, S1 (2009) [arXiv:0809.1869 [hep-ex]].
1460
- 1461 [93] M. Gersabeck *et al.* [LHCb Collaboration], arXiv:1209.5878 [hep-ex].
- 1462 [94] B. I. Eisenstein *et al.* [CLEO Collaboration], Phys. Rev. D **78**, 052003 (2008) [arXiv:0806.2112 [hep-ex]].
- 1463 [95] G. Rong, arXiv:1209.0085 [hep-ex].
- 1464 [96] A. Zupanc *et al.* [Belle Collaboration], arXiv:1212.3942 [hep-ex].

- 1465 [97] A. S. Kronfeld, arXiv:0912.0543 [hep-ph].
- 1466 [98] R. Aaij *et al.* [LHCb Collaboration], Phys. Rev. Lett. **110**, 101802 (2013) [arXiv:1211.1230 [hep-ex]].
- 1467 [99] A. F. Falk, Y. Grossman, Z. Ligeti and A. A. Petrov, Phys. Rev. D **65**, 054034 (2002) [hep-ph/0110317];
1468 A. F. Falk, Y. Grossman, Z. Ligeti, Y. Nir and A. A. Petrov, Phys. Rev. D **69**, 114021 (2004) [hep-
1469 ph/0402204].
- 1470 [100] E. Golowich, J. Hewett, S. Pakvasa and A. A. Petrov, Phys. Rev. D **76**, 095009 (2007) [arXiv:0705.3650
1471 [hep-ph]].
- 1472 [101] O. Gedalia, Y. Grossman, Y. Nir and G. Perez, Phys. Rev. D **80**, 055024 (2009) [arXiv:0906.1879
1473 [hep-ph]]. M. Ciuchini *et al.*, Phys. Lett. B **655**, 162 (2007). [arXiv:hep-ph/0703204].
- 1474 [102] M. Artuso, B. Meadows and A. A. Petrov, Ann. Rev. Nucl. Part. Sci. **58**, 249 (2008); A. Ryd and
1475 A. A. Petrov, Rev. Mod. Phys. **84**, 65 (2012); S. Bianco, F. L. Fabbri, D. Benson and I. Bigi, Riv. Nuovo
1476 Cim. **26N7**, 1 (2003); [arXiv:hep-ex/0309021]. G. Burdman and I. Shipsey, Ann. Rev. Nucl. Part. Sci.
1477 **53**, 431 (2003); X. Q. Li, X. Liu and Z. T. Wei, Front. Phys. China **4**, 49 (2009).
- 1478 [103] I. I. Bigi, arXiv:0902.3048 [hep-ph].
- 1479 [104] R. Aaij *et al.* [LHCb Collaboration], Phys. Rev. Lett. **108**, 111602 (2012); T. Aaltonen *et al.* [CDF
1480 Collaboration], Phys. Rev. Lett. **109**, 111801 (2012); New measurements do not confirm those results:
1481 R. Aaij *et al.* [LHCb Collaboration], Phys. Lett. B **723**, 33 (2013);
- 1482 [105] M. Golden and B. Grinstein, Phys. Lett. B **222**, 501 (1989); J. Brod, A. L. Kagan and J. Zupan,
1483 Phys. Rev. D **86**, 014023 (2012); B. Bhattacharya, M. Gronau and J. L. Rosner, Phys. Rev. D **85**,
1484 054014 (2012); I. I. Bigi and A. Paul, JHEP **1203**, 021 (2012); G. Isidori, J. F. Kamenik, Z. Ligeti
1485 and G. Perez, Phys. Lett. B **711**, 46 (2012); J. Brod, Y. Grossman, A. L. Kagan and J. Zupan,
1486 JHEP **1210**, 161 (2012); W. Altmannshofer, R. Primulando, C. -T. Yu and F. Yu, JHEP **1204**, 049
1487 (2012); Y. Grossman, A. L. Kagan and J. Zupan, Phys. Rev. D **85**, 114036 (2012); H. -Y. Cheng
1488 and C. -W. Chiang, Phys. Rev. D **85**, 034036 (2012) [Erratum-ibid. D **85**, 079903 (2012)]; G. Hiller,
1489 Y. Hochberg and Y. Nir, Phys. Rev. D **85**, 116008 (2012); T. Feldmann, S. Nandi and A. Soni, JHEP
1490 **1206**, 007 (2012).
- 1491 [106] E. Golowich, J. Hewett, S. Pakvasa and A. A. Petrov, Phys. Rev. D **79**, 114030 (2009).
- 1492 [107] D. Atwood and A. Soni, Phys. Rev. D **68**, 033003 (2003) [hep-ph/0304085].
- 1493 [108] N. Brambilla, S. Eidelman, B. K. Heltsley, R. Vogt, G. T. Bodwin, E. Eichten, A. D. Frawley and
1494 A. B. Meyer *et al.*, Eur. Phys. J. C **71**, 1534 (2011) [arXiv:1010.5827 [hep-ph]].
- 1495 [109] M. Ablikim *et al.* [BESIII Collaboration], arXiv:1303.5949 [hep-ex].
- 1496 [110] G. Pakhlova *et al.* [Belle Collaboration], Phys. Rev. Lett. **101**, 172001 (2008) [arXiv:0807.4458 [hep-
1497 ex]].
- 1498 [111] T. Blum *et al.* [USQCD Collaboration], *Lattice QCD at the Intensity Frontier*, [http://www.usqcd.
1499 org/documents/13flavor.pdf](http://www.usqcd.org/documents/13flavor.pdf) (2013).
- 1500 [112] R. Brower *et al.* [USQCD Collaboration], *Fundamental parameters from future lattice calculations*,
1501 <http://www.usqcd.org/documents/fundamental.pdf> (2007).
- 1502 [113] J. Laiho, E. Lunghi and R. S. Van de Water, Phys. Rev. D **81**, 034503 (2010) [arXiv:0910.2928 [hep-
1503 ph]].
- 1504 [114] G. Colangelo *et al.* [FLAG], Eur. Phys. J. C **71**, 1695 (2011) [arXiv:1011.4408 [hep-lat]].
- 1505 [115] T. Blum *et al.* [RBC and UKQCD Collaborations], Phys. Rev. Lett. **108**, 141601 (2012)
1506 [arXiv:1111.1699 [hep-lat]].
- 1507 [116] T. Blum *et al.* [RBC and UKQCD Collaborations], Phys. Rev. D **86**, 074513 (2012) [arXiv:1206.5142
1508 [hep-lat]].

- 1509 [117] P. A. Boyle *et al.* [RBC and UKQCD Collaborations], arXiv:1212.1474 [hep-lat].
- 1510 [118] N. H. Christ *et al.* [RBC and UKQCD Collaborations], Phys. Rev. Lett. **105**, 241601 (2010)
1511 [arXiv:1002.2999 [hep-lat]].
- 1512 [119] P. Junnarkar and A. Walker-Loud, arXiv:1301.1114 [hep-lat].
- 1513 [120] N. H. Christ, T. Izubuchi, C. T. Sachrajda, A. Soni and J. Yu [RBC and UKQCD Collaborations],
1514 arXiv:1212.5931 [hep-lat].
- 1515 [121] L. Lellouch and M. Luscher, Commun. Math. Phys. **219**, 31 (2001) [hep-lat/0003023].
- 1516 [122] T. Blum *et al.* [RBC and UKQCD Collaborations], Phys. Rev. D **84**, 114503 (2011) [arXiv:1106.2714
1517 [hep-lat]].
- 1518 [123] C. Kelly *et al.* [RBC and UKQCD Collaborations], PoS LATTICE **2012**, 130 (2012).
- 1519 [124] J. Brod and M. Gorbahn, Phys. Rev. D **82**, 094026 (2010) [arXiv:1007.0684 [hep-ph]].
- 1520 [125] V. Cirigliano, G. Ecker, H. Neufeld, A. Pich and J. Portoles, Rev. Mod. Phys. **84**, 399 (2012)
1521 [arXiv:1107.6001 [hep-ph]].
- 1522 [126] M. T. Hansen and S. R. Sharpe, Phys. Rev. D **86**, 016007 (2012) [arXiv:1204.0826 [hep-lat]].
- 1523 [127] S. -W. Qiu *et al.* [Fermilab Lattice and MILC Collaborations], PoS LATTICE **2011** (2011) 289
1524 [arXiv:1111.0677 [hep-lat]].
- 1525 [128] J. P. Lees *et al.* [BaBar Collaboration], Phys. Rev. Lett. **109**, 101802 (2012) [arXiv:1205.5442 [hep-ex]].
- 1526 [129] J. A. Bailey *et al.* [Fermilab Lattice and MILC Collaborations], Phys. Rev. Lett. **109**, 071802 (2012)
1527 [arXiv:1206.4992 [hep-ph]].
- 1528 [130] C. McNeile, C. T. H. Davies, E. Follana, K. Hornbostel and G. P. Lepage [HPQCD Collaboration],
1529 Phys. Rev. D **85**, 031503 (2012) [arXiv:1110.4510 [hep-lat]].
- 1530 [131] R. Zhou, arXiv:1301.0666 [hep-lat].
- 1531 [132] W. Detmold, C. -J. D. Lin, S. Meinel and M. Wingate, Phys. Rev. D **87**, 074502 (2013) [arXiv:1212.4827
1532 [hep-lat]].
- 1533 [133] I. Baum, V. Lubicz, G. Martinelli, L. Orifici and S. Simula, Phys. Rev. D **84**, 074503 (2011)
1534 [arXiv:1108.1021 [hep-lat]].